Fundamental Value Pricing and Bubbles for Nontraditional Assets: The Case of Cryptocurrencies[*]

Rustam Ibragimov[†]   Christine A. Parlour[‡]   Johan Walden[§]

Abstract

We study the fundamental value pricing relationship for nontraditional assets, for which yields and rare event crash risk are unobservable, and not well understood. We introduce a novel test for deviations from fundamental value pricing for such assets. Simulations show that our test performs well for some benchmark examples that bubble tests based on unit roots or explosive behavior may find hard to handle. For traditional stocks and stock indexes, our test typically does not detect bubbles. When applied to cryptocurrencies, our test suggests the presence of a bubble for multiple large cryptocurrencies at risk adjusted discount rates up to 25% per year, and even at 50% per year. For Ethereum, extremely high risk adjusted discount rates, above 71% per year, are needed for our test to fail to reject the no-bubble null hypothesis. For Stellar, the null is rejected even at the very high risk adjusted discount rate of 100% per year.

Keywords: Bubbles, fundamental value, intrinsic value, cryptocurrencies.

1   Introduction

Financial innovation necessitates the creation of new assets. Such assets are difficult to value from fundamentals, and have a limited trading history. In such assets, identifying when the price differs from the fundamental (intrinsic) value is difficult but very important. In other words, how can one identify bubbles in innovative assets? In this paper we propose a flexible bubble test that can be applied to such assets. A natural application of our new test is to cryptocurrencies. First, there is considerable uncertainty about the determinants of value for cryptocurrencies. Comparing Bitcoin to a bubble and a Ponzi scheme, economist Paul Krugman ended his January 29, 2018, op-ed article with "This will end badly, and the sooner it does, the better,"[1] a view in line with the market value of Bitcoin deviating from its fundamental value. Second, over the last decade large and liquid markets for cryptocurrencies have developed and so traded price sequences are available for many of these cryptoassets, although over a limited time period.

The key to our test is that while we observe price dynamics, we do not observe the use value of the assets or the risk of rare catastrophic events that have not yet been realized. In other words, there may be significant "Peso risk" present. This is a major challenge for bubble tests that are based on parametric specification of such processes. By contrast, we use a parsimonious asset pricing framework that makes minimal assumptions about these processes. Notably, we make no assumption about how they vary over time. This is important as time variation in these processes may lead to prices that exhibit bubble-like behavior (e.g., rapid rises) even though prices accurately reflect fundamental values.

We provide several examples for which our tests identify bubbles accurately, while parametric approaches fail. Further, in simulated economies we show that our approach is robust and conservative. Specifically, it almost always avoids falsely rejecting the no-bubble hypothesis (Type I errors) while correctly identifying bubbles in most cases when they are present. As an empirical exercise, we apply our test to some large cryptocurrencies. For BitCoin, Dogecoin, and several other cryptocurrencies, price dynamics are consistent with fundamental pricing according to our test, whereas for Ethereum and Stellar the presence of bubbles are strongly suggested.

To understand our framework, consider the following simple asset pricing formulation. The fundamental value of an asset is defined as the present value of the discounted cash flows it is expected to generate in the future. In a continuous time setting, this is simply expressed as

$$V_t \stackrel{\text{def}}{=} E_t \left[\int_t^T e^{-r(z-t)} S_z dz + e^{-r(T-t)} P_T \right]. \tag{1}$$

---

[1]Paul Krugman, "Bubble, Bubble, Fraud and Trouble," Op-Ed, New York Times, January 29, 2018.

Here, S_t represents the instantaneous benefit, the *surplus flow*, received when owning the asset at t, and r is the risk adjusted discount rate. In the absence of a bubble, the market value of the asset, P_t, i.e., the price it trades at in the market, equals its fundamental value

$$P_t = V_t, \quad \text{for all } t \leq T.$$

If $P_t > V_t$ at any point, then a bubble is present at t. If $P_t < V_t$, an inverse bubble is present. We jointly denote any observation of $P_t \neq V_t$ a bubble.

In differential form, the pricing relation of Equation (1) becomes

$$E\left[dP_t\right] = rP_t dt - S_t dt, \tag{2}$$

or, equivalently, defining the yield as $y_t \overset{\text{def}}{=} \frac{S_t}{P_t}$,

$$E\left[\frac{dP_t}{P_t}\right] = (r - y_t)dt. \tag{3}$$

If observed price dynamics of an asset are consistent with fundamental prices, (i.e., $P_t = V_t$ for all t), they will be consistent with (3). If price dynamics are inconsistent with (3), then there must be a bubble. Our focus in this paper is on studying whether (3) is violated.

Although the relation presented in Equation (3) is consistent with fundamental value pricing, in an infinite horizon setting it may also be consistent with the presence of a rational bubble (see, e.g., Blanchard 1979, and Froot and Obstfeld 1991).[2] Our focus is not to distinguish between rational bubbles and fundamental value pricing. We therefore study a finite horizon setting, assuming a finite terminal date far into the future, $T < \infty$, at which point the asset makes its final payment, F_T, and seizes to exist. In this case, the fundamental value pricing relation becomes:

$$P_t = E_t\left[\int_t^T e^{-r(z-t)} S_z dz + e^{-r(T-t)} F_T, \right]. \tag{4}$$

which is necessary and sufficient for the absence of bubbles, and equivalent to the condition that Equation (3) holds at all points in time $t < T$, together with the terminal condition $P_T = F_T$. Our finite horizon specification also means that our approach will in general not detect a bubble in an asset that acts as a store of value by fiat (whether through government backing as for traditional currencies,

---

[2]We conduct our analysis in a homogeneous beliefs setting, in which there is agreement about the expectation in (1). In heterogeneous beliefs models, bubbles may also arise in finite horizon settings with rational agents under some fairly strong conditions (private information, short sale constraints and lack of common knowledge of trades), see Allen et al. (1993). Our focus on models with homogeneous beliefs, rules out such bubbles.

or via other mechanisms).

For many assets, such as the equity claims on a publicly traded company, the values of the yield, y_t, the risk adjusted discount rate r, and the dynamics of dP_t are known or observed. Specifically, the price P_t is observed, the surplus, S_t, is captured by periodic dividend payments (and thereby also the yield, y_t) and the risk adjusted discount rate, r, can be estimated from an asset pricing model (e.g., the Capital Asset Pricing Model). Finally, the dynamics of dP_t are easily measured from traded prices.

For other assets less information is available. New companies have limited price and return observations, may yet have not made a single dividend payment, and often have negative earnings. In such cases, valuation may be inferred from the historical performance of comparable mature firms within the same industry. Occasionally, the surplus flow may not be observed, but still inferred; for example, the convenience yield on some commodities is not observed, but the properties and determinants of such yields are well understood and so empirical proxies are available. For other assets, such empirical proxies may not be known.

Our test is most useful for *nontraditional assets*, for which the surplus process S_t is both unobservable and not necessarily universally agreed on. Indeed, there may be competing explanations what the surplus flow represents. Moreover, for these nontraditional asset there are limited historical observations of the price process. Of course, limited time series make accurate estimates on the presence and frequency of rare events challenging.

Our test is general, but we focus on cryptocurrencies as they provide a natural application. For cryptocurrencies, there are competing explanations for what the surplus represents and its magnitude.[3] Moreover, cryptocurrencies may be exposed to rare event risk that have not yet been realized; new regulation or technological problems. To capture this risk, we consider a small risk per unit time, λ_t, that the cryptocurrency instantaneously becomes obsolete, crashes, and loses all of its value. Until the event occurs, it is unobserved, but the risk still affects price dynamics in a rational market. For (3) to hold under the presence of such risk, realized returns must be higher than they would be in its absence (to make up for the loss if the crash eventually arrives). For a traditional asset, such crash risk may also be present, but given that the asset has a long history of observations, it must likely be very small in each period; otherwise a crash would most likely have already occurred and the asset would already be worthless. For an asset with limited history, the per period crash risk may be significant while the cumulative risk that that a crash has arrived is still modest.

Our goal is to study whether observed price dynamics of a nontraditional asset are consistent

---

[3]We defer a discussion of these until we introduce our empirical tests.

with (3), while making as few assumptions as possible about the yield and crash processes, y_t and λ_t. The assumptions we impose are that the econometrician sets an upper bound on the sample averages of these processes over the period of study, and also an upper bound on the risk adjusted discount rate r. The restriction on λ_t is very natural since it is directly related to the cumulative crash probability over the observation period. The upper bound on the yield, y_t, could, for example, arise if the econometrician has an idea about the possible sources of the surplus, choosing the maximum among the competing explanations.

Our approach is in the spirit of the literature on Peso problems, with respect to the unobserved crash risk part of the model, see Rogoff (1977, 1980), Krasker (1980), Lizondo (1983), and Kaminsky (1993). This literature explains apparent deviations from efficiency in forward exchange markets by rare events that have yet not occurred, e.g., devaluations. For example, Krasker (1980), using a linear specification of the crash risk process, λ_t, showed that efficiency in the mark/pound forward rate during the German hyperinflation era, from January 1921 to September 1923, could not be rejected when taking into account the possibility for sudden stabilization of the German mark. We deviate from these approaches in making no assumptions about the functional form of the crash risk processes, by incorporating unobserved surplus yields, and by incorporating time-varying volatility. This allows us to analyze general nontraditional assets, going beyond the dynamics of currency forward rates.

1.1 Related literature on bubbles and mispricing

Many papers in econometrics, time series analysis, empirical finance and related fields have focused on the development and applications of econometric tests for identification of bubbles. Following Phillips et al. (2011), most of the approaches to testing for bubbles in financial and economic time series in econometrics focus on identifying explosive behavior in the time series, in the form of the autoregressive coefficient being greater than one in autoregression approximations. Specifically, in this framework the null hypothesis of a unit root (the autoregressive coefficient equals one) in autoregression approximations to the time series of log prices is tested against the alternative of explosive behavior, in terms of the autoregressive coefficient being graters than one.

Phillips et al. (2011) propose a sup augmented Dickey-Fuller, sup-ADF (SADF), statistic for testing for the presence of explosive behavior in time series dealt with. A number of papers deal with extensions of the approaches proposed in Phillips et al. (2011) and develop tests for explosive behavior in autoregressive processes under wide range of model specifications such as inclusion of time trend and assumptions on the structure of time series dependence in the autoregression errors, including time-varying volatility (see Phillips et al. (2014), Harvey et al. (2016), Harvey et al. (2018), Harvey

et al. (2020) and the discussion therein). Phillips et al. (2015a, 2015b) propose Generalized Supremum ADF (GADF) statistics for testing for multiple explosive regimes in time series and provide inference approaches for dating bubble periods.

Several papers have focused on applications of the econometric approaches to testing for explosive behavior in detection of bubbles in important economic and financial time series, including asset prices (see the aforementioned papers), cryptocurrency prices (e.g., Astill et al. (2021), Cheah and Fry (2015), Harvey et al. (2020)), housing and commodity prices, foreign exchange rates and others (see Shi and Phillips (2021) and Skrobotov (2021) for a review of approaches to bubble/explosive time series behavior and their empirical applications).

Our paper, being based on the fundamental value pricing relation (4), takes a different approach, as we shall see.

1.2 The Fundamental Value of a Cryptocurrency

Cryptocurrencies are not traditional assets as they are frequently not claims to underlying cash flows, and there have been various investigations into the source of their value. One of first papers to develop a fundamental valuation model of Bitcoin is Athey et al. (2016). This paper uses a rational expectations framework and the use of Bitcoin as a payments medium to analyze value dynamics. Following this, there has been a strand of literature that focuses on the payments role of Bitcoin as its source of value. Among others, Pagnotta and Buraschi (2018) build a model to analyze the fundamental value of Bitcoin and other blockchain tokens, while Foley et al. (2019) emphasize how Bitcoin could be used in illegal activities and hence be valuable for a segment of the population. Fundamental uses of Bitcoin seem to be tied to its use as payments, however, as documented in Schuh and Shy (2015), there has not been global adoption.

Various papers have postulated a relationship between cryptocurrencies and the size of the network on which they operated. The idea here is that cryptocurrencies are the medium of exchange on a platform and so their value is intimately tied to platform adoption and use. For example, Cong et al. (2021) develop a theoretical model with endogenous user adoption, in which network effects cause the cryptocurrency's value to be increasing in adoption rates, and calibrate their model to the value and adoption rates of 16 currencies between 2010 and 2018. Similarly, Sockin and Xiong (2018) considers how the use value of a cryptocurrency translates into a market value.

Other papers consider cryptocurrencies as a bundle of attributes including store of value, medium of exchange and also the potential exposure to hack or collapse risk. Such a fundamental valuation is estimated by Biais et al. (2020), while Pagnotta (2022) emphasizes the importance of security in

valuing cryptocurrencies.

The prevalence of market prices for cryptocurrencies has encouraged a rapidly growing literature. Some authors have stressed that observed prices could be due to manipulation. Gandal et al. (2018), studying suspicious trading activity on the Mt. Gox Bitcoin currency exchange, find evidence of periods when Bitcoin's price was subject to market manipulation. Issues with cross market prices have also been documented in Makarov and Schoar (2020), while Choi et al. (2018) document a premium due to regulation. In an interesting article, Griffin and Shams (2018) suggest demand for Bitcoin might be endogenous and inflated. Liu and Tsyvinsky (2021) study the return dynamics of three cryptocurrencies (Bitcoin, Ripple, and Ethereum), and verify that they are different than those of other asset classes (stocks, currencies, commodities), in line with our model assumptions. Further Urquhard (2016) suggests in several tests that Bitcoin violates weak form market efficiency, for example showing return anti-persistence.

2 Model

Time is continuous, $t \geq 0$. The fundamental value of a nontraditional asset equals

$$V_t = E_t \left[\int_t^{\tau \wedge T} e^{-r(z-t)} S_z dz + 1_{\tau_t < T} e^{-r(T-t)} F_T \right], \tag{5}$$

Here, $\tau \leq \infty$ represents the time of an observable crash event, that immediately makes the asset worthless if it occurs before the terminal date, T. As discussed in the introduction, the terminal date lies in the far future, at which point the asset — if alive at that point— makes the payment F_T and seizes to exist. Here r is a risk adjusted discount rate for the type of risk, which we assume is constant. The expectation is thus taken with respect to the physical (not risk neutral) measure, and risk premia are accounted for by risk adjusting the discount rate, as in several standard asset pricing models. The asset is traded in the market, at price P_t. If $P_t = V_t$ for all t, then the price reflects fundamental value. Otherwise, a bubble is present. The fundamental value yield process is $y_t = \frac{S_t}{V_t}$.

Note that the yield may be very low (or even zero) for a long time, even until the terminal date T, which may in turn lie far into the future. For a cryptocurrency, this suggests that its use value may not necessarily be high now or in the near future, even if the asset is very valuable and even if there is a bubble. For example, the current value may be derived from a small but nonnegligible chance that the cryptocurrency will eventually (at F_T) replace the dollar as the world currency, in which case it will become tremendously valuable. Large swings in the fundamental valuate (5) may then occur if new information arrives that makes the market revise the likelihood that the replacement will

7

eventually happen.

The crash-time τ is determined by the first jump of the counting process J_t, with unobservable time-varying and stochastic intensity. The value, crash, and yield processes are adapted to the filtered probability space $(\Omega, \mathcal{F}, \mathbb{P}, \{\mathcal{F}_t\}_t)$, carrying the counting process J_t with predictable stochastic intensity λ_t, and a Wiener process W_t, and where the filtration $\{\mathcal{F}_t\}_t$ is the internal one. Note that the discounted value process $e^{-rt}V_t$ is an $\mathcal{F}_t$-martingale. It therefore follows from a martingale representation theorem for jump diffusion processes, see Bjork (2011), that V_t has the representation

$$\frac{dV_s}{V_s} = (r + \lambda_s - y_s)ds + \sigma_s dW_s - dJ_s, \tag{6}$$

for some adapted volatility process σ_s, where we assume σ_s is bounded, i.e., $\sigma_s \leq \bar{\sigma}$. Moreover, we assume that λ_t and σ_t have continuous sample paths (almost surely). Finally, we assume that dJ_s and dW_s are independent. Implicit in (6) is the assumption that dJ_s risk is not associated with a risk-premium, for example, representing idiosyncratic risk. This is in line with the assumptions made in Merton (1976).

Our specification, with only downward jumps that lead to a complete value destruction, may see quite specific. However, the specification is natural in that it is the one that maximally "ties our hands" how much one may explain explaining bubble-like behavior by unobserved rare event risk. Unobserved upward jumps would pull down observed returns while not being realized, just like unobserved crash risk pushes them up. As a consequence, incorporating such upward jumps woul therefore all else equal lead to a higher inferred increase the likelihood of bubbles. Our approach is to study the "strongest case against the presence of bubbles," and we therefore do *not* include upward jumps in the specification.

Note that the effect on returns in (6) due to unobserved instantaneous crash risk (λ_s) is always positive. There may also be innovations at time s about future crash risk, i.e., about λ_t, $t > s$. Such innovation can have either a positive or negative effect on the asset's price. If future crash risk increases, the current spot price decreases, and if it decreases the current price increases. In our model, such innovation about future crash risk would be captured as a component of the dW_s term, whereas the event $dJ_s = 1$ captures an actual crash at t.

Also note that conditioned on $s < \tau$ (so that $J_s = 0$), it follows from (6) that

$$E\left[\frac{dV_s}{V_s} \,\middle|\, s < \tau\right] = (r + \lambda_s - y_s)dt. \tag{7}$$

The difference between (3) and (7) is that the latter expression takes into account a survivorship bias

effect, from knowledge about the fact that the asset does not not crash at s (or before).

The cumulative probability that the asset has survived until t is

$$L_t = e^{-t\bar{\lambda}_t}, \qquad \text{where } \bar{\lambda}_t = \frac{1}{t} \int_0^t \lambda_s ds.$$

The average convenience yield up until t is

$$\bar{y}_t = \frac{1}{t} \int_0^t y_s ds.$$

Our null hypothesis, that we wish to test, is that $P_s = V_s$ for all s. The price dynamics $\{P_s\}_s$, $0 \le s \le t$, are observed until time $t < \tau$, so $J_t = 0$. Because of standard results on the quadratic variation of a Wiener process, it follows that $\{\sigma_s\}_s$ is observable for $0 \le s \le t$. Moreover, per assumption, the risk adjusted discount r is also known, or at least a bound $r \le \bar{r}$ is known, e.g. being determined by a trusted asset pricing model.

For a nontraditional asset, the processes $\{\lambda_s\}_s$ and $\{y_s\}_s$ are not observed. For a traditional asset, which has been traded for a long time, $\bar{\lambda}_t$ is likely very small, since L_t would otherwise be small and the asset would most likely have crashed by t. Similarly, for a traditional asset, the yield y_s is either observed (as for a plain vanilla stock) or at least well understood (as convenience yields are for commodities). Here, such inferences are not available. Indeed, short-term run-ups in prices could potentially be explained by high λ_s, and short-term run-downs by high y_t.

The unobservability of the yield makes several traditional methods infeasible. For example, to apply methods that detect bubbles based on abnormal yields (or inverse yields), see Shiller (2000, 2014), indirect methods of measuring the surplus are needed which makes such approaches challenging in this environment. Applying various methods based on excess volatility, see Shiller (1981), would also be challenging, since it requires frequent observations of the yield.

We wish to make as few restrictions as possible on $\{\lambda_s\}_s$ and $\{y_s\}_s$, but with no limitations there is little one can infer about whether the price process is consistent with fundamental value. Our assumption is therefore that the econometrician knows very little about their local dynamics, except for that they are both nonnegative and bounded. Moreover, (s)he knows an upper bound on their sample averages during the observation period:

$$\bar{\lambda}_t \le \bar{\lambda},$$
$$\bar{y}_t \le \bar{y}.$$

9

For example, the econometrician may view it as highly unlikely that $L_t < 0.05$, which would correspond to a 95% or higher likelihood that the asset would have crashed by t. This then implies that $\bar{\lambda}_t \leq -\frac{\ln(0.05)}{t}$. Similarly, arguments based on first principles may suggest that the average yield should have an upper bound, for example, 15% per year.

Definition 1. *The Consistency Verification Problem (CVP) is defined as follows: Given observations of $\{P_s\}_s$ and $\{\sigma_s\}_s$ for the period $0 \leq s \leq t$ during which $J_s = 0$, do there exist parameters $(r, \bar{\lambda}_t, \bar{y}_t) \in \Gamma \stackrel{\text{def}}{=} [\underline{r}, \bar{r}] \times [0, \bar{\lambda}] \times [0, \bar{y}]$, so that the observed dynamics $\{P_s\}_s$ are well explained by the process for $\{V_s\}_s$, as defined by (6)?*

We denote Γ the consistency set, and the CVP then addresses whether there are values of r, $\bar{\lambda}_t$, and $\bar{y}_t$ in this set, such that observed dynamics are consistent with fundamental values.

Implicit in our model is the assumption that the asset's market risk does not depend on its volatility, i.e., r does not depend on σ_t. This corresponds to assets for which the volatility variation over time is exclusively caused by idiosyncratic risk. An alternative specification allows the variation to depend on market risk, in which case

$$\frac{dV_s}{V_s} = (r^f + \rho \eta \sigma_s + \lambda_s - y_s)ds + \sigma_s dW_s - dJ_s. \tag{8}$$

Here, ρ denotes the correlation of the asset's return and the market's returns. Specifically, the market risk process is governed by a Wiener process W^m, such that $\langle dW, dW^m \rangle = \rho\, dt$, r^f is the risk-free rate, and $\eta = \frac{r^m - r^f}{\sigma^m}$ is the market's Sharpe ratio. Both ρ and r^f may in principle vary over time. In this setting, we would still assume that the crash risk is idiosyncratic.

We focus on the idiosyncratic variation of volatility with constant r, i.e., the specification defined by (6), which we denote the *base specification*. But the analysis is identical under the alternative specification (8), which we denote the Sharpe ratio specification. For robustness, we also do tests using the *Sharpe ratio specification*.

We have so far developed the model in continuous time, which makes the arguments straightforward and tractable. However, empirical tests are based on discrete observations, e.g., at weekly or daily horizons. We therefore specify the discrete version of the CVP.

2.1 Discrete Consistency Verification Problem (CVP)

Consider discrete observations of returns

$$\mu_n = \frac{P_{(n+1)\Delta t} - P_{n\Delta t}}{P_{n\Delta t}}, \qquad n = 0, 1, \ldots, N-1.$$

define $\lambda_n = \lambda_{n\Delta t}\Delta t$, $y_n = y_{n\Delta t}\Delta t$, $\sigma_n = \sigma_{n\Delta t}\sqrt{\Delta t}$, $n = 0, 1, \ldots, N - 1$. For small Δt, the following approximate discrete relationship then holds

$$\mu_n = u + \lambda_n - y_n + \sigma_n \xi_n, \tag{9}$$

where ξ_n are i.i.d., standard normally distributed, $\xi_n \sim N(0, 1)$, and where $u = r\Delta t$.[4] Moreover, the bounds on average crash intensity and yield in the discrete setting map like $\bar{\lambda} \mapsto \bar{\lambda}\Delta t$ and $\bar{y} \mapsto \bar{y}\Delta t$. For large N, it follows from the Glivenko-Cantelli theorem that the empirical distribution function of $\{\xi_n\}_n$ is close to that of the normal distribution function (in the maximum norm). This leads us to

Definition 2 (Discrete CVP). *Consider the observed processes μ_n and σ_n, $n = 1, 2, \ldots, N$, and the consistency set $\Gamma \overset{\text{def}}{=} [\underline{u}, \bar{u}] \times [0, \bar{\lambda}] \times [0, \bar{y}]$. These observations are said to be* consistent with fundamental values *if there exists a triplet $(u, \lambda, y) \in \Gamma$, a sequence ξ_n, $n = 1, \ldots, N$, and two nonnegative sequences λ_n and y_n, $n = 0, \ldots, N - 1$, such that*

1. $\mu_n = u + \lambda_n - y_n + \sigma_n \xi_n$, $n = 0, \ldots, N - 1$

2. $\lambda = \frac{1}{N}\sum_n \lambda_n$, and $y = \frac{1}{N}\sum_n y_n$,

3. The empirical distribution function associated with $\{\xi_n\}_n$, F_ξ, is approximately that of a standard normal distribution, Φ: $\|F_\xi - \Phi\|_\infty < \epsilon(N)$, for some function $\epsilon(N) \to_{N \to \infty} 0$.

2.2   Solving the discrete CVP

To solve the discrete CVP, we proceed as follows: For a given u, we define

$$q_n = \mu_n - u,$$

which given knowledge of u is observable, and the sequence

$$G_s = \Phi^{-1}\left(\frac{s + 1}{N + 1}\right), \qquad s = 0, \ldots, N - 1, \tag{10}$$

where Φ is the cumulative distribution function of the standard normal distribution.

We now find the nonnegative sequences $\{\lambda_n\}_n$ and $\{y_n\}_n$ with the minimal averages values, λ and y, such that the sequence

$$x_n = \frac{q_n - \lambda_n + y_n}{\sigma_n},$$

---

[4]Under the Sharpe ratio representation, we would replace u with $u_n = (r^f + \rho_{n\Delta t}\eta\sigma_{n\Delta t})\Delta t$.

is approximately i.i.d. normally distributed, in that its empirical distribution function coincides with G. Specifically, for each permutation $\Pi : \{0, \ldots, N-1\} \leftrightarrow \{0, \ldots, N-1\}$, we calculate the minimal average realizations of $\{\lambda_n\}_n$ and $\{y_n\}_n$, such that

$$G_{\Pi(n)} = x_n, \qquad n = 0, \ldots, N-1.$$

Among all permutations, we then choose the one choose, Π, that minimizes these averages.

We can find the solution by solving a linear programming problem. Specifically, define the cost function

$$C_{n,m} = \alpha \max(q_n - \sigma_n G_m, 0) + (1 - \alpha) \max(\sigma_n G_m - q_n, 0), \qquad \alpha \in [0, 1].$$

This is the "cost" of associating the nth observation of returns with the mth largest observation of ξ_n as defined in (10), $\xi_n = G_m$, either by λ_n contributing to making the average λ larger (if $q_n - \sigma_n \xi_n > 0$), or by y_n contributing to making the average y larger (if $q_n - \sigma_n \xi_n < 0$).

When $\alpha = 1/2$, the weight on λ and y in this optimization problem is the same. When α is close to 1, almost all weight is put on λ, making it more costly to increase λ than y, and when α is close to 0, almost all weight is put on y, making it more costly to increase y. We will mainly use $\alpha = 1/2$, putting equal weight on λ and y, which works well in simulations.

Solving the CVP then boils down to solving

$$\min_{\{X_{nm}\}_{n,m}} \sum_{n,m=0}^{N-1} C_{nm} X_{nm}, \text{ s.t.} \tag{11}$$

$$X_{nm} \in \{0, 1\}, \quad n, m = 0, \ldots, N-1, \tag{12}$$

$$\sum_m X_{nm} = 1, \qquad n = 0, \ldots, N-1, \tag{13}$$

$$\sum_n X_{nm} = 1, \qquad m = 0, \ldots, N-1. \tag{14}$$

This problem can be solved in polynomial time using standard methods, e.g., with the so-called Hungarian algorithm. Here, $X_{nm} = 1$ means that the nth observation, q_n, is associated with the realization $\xi_n = G_m$, i.e., that $\Pi(n) = m$. The associated values of λ_n and y_n that minimize average λ and y are then

$$\lambda_n = \max\left(q_n - \sigma_t G_{\Pi(n)}, 0\right),$$
$$y_n = \max\left(\sigma_n G_{\Pi(n)} - q_n, 0\right),$$

12

and

$$\lambda = \frac{1}{N} \sum_{n=0}^{N-1} \lambda_n, \qquad y = \frac{1}{N} \sum_{n=0}^{N-1} y_n,$$

with the associated estimated crash risk

$$\hat{L} = e^{-\lambda^N T}.$$

If $\lambda \leq \bar{\lambda}$ and $y \leq \bar{y}$, then (u, λ, y) is a solution to the CVP. We also define $(\lambda, y) = CVP(u, \alpha) = CVP(u, \alpha; \{\mu_n\}_n, \{\sigma_n\}_n)$, as the average crash risk and yield associated with the solution to (11-14) under observations $\{\mu_n\}_n$, and $\{\sigma_n\}_n$. If no such solution $(u, \lambda, y) \in \Gamma$ exists, then we conclude that the observed price dynamics is not consistent with fundamental value pricing.

The CVP method takes the most conservative possible approach when studying the impact of $\{\lambda_n\}_n$ and $\{y_n\}_n$, assuming that they are high in exactly the periods that makes price dynamics seem as removed from fundamental pricing as possible (when not taken into account crash risk and yields). We have

Proposition 1. *Consider the fundamental value process (6). For large N, the solution to the CVP, $(\lambda^N, y^N) = CVP(u, \alpha)$, satisfies*

$$\alpha \lambda^N + (1 - \alpha) y^N \leq \alpha \bar{\lambda}_{N\Delta t} + (1 - \alpha) \bar{y}_{N\Delta t} + o_p(1), \tag{15}$$

where the left-hand-side represents estimated sample averages from the CVP, and the right-hand-side represents actual sample averages.

Moreover, consider the sequences $\{\lambda_n^N\}_n$ and $\{y_n^N\}_n$ associated with the solution $(\lambda^N, y^N) = CVP(u, 1/2)$, and the sequence

$$\hat{\xi}_n = \frac{\mu_n - u - \lambda_n^N + y_n^N}{\sigma_n},$$

$n = 0, \ldots, N - 1$. Define

$$Q^N \stackrel{\text{def}}{=} \frac{1}{N} \sum_{n=0}^{N-1} \sigma_n \hat{\xi}_n.$$

Then, if $\lambda_n y_n = 0$ for all n,

$$\bar{\lambda}_{N\Delta t} \leq \lambda^N + y^N + \bar{y} + Q^N + o_p(1). \tag{16}$$

In the general case, when it may be that $\lambda_n y_n > 0$, the following inequality holds:

$$\bar{\lambda}_{N\Delta t} \leq \lambda^N + y^N + 3\bar{y} + Q^N + o_p(1). \tag{17}$$

13

From the upper bound (15), we conclude that for large N, if there is no solution to the CVP that is consistent with the reasonable range of average crash risk and average yield, then prices do not reflect fundamental values, since the actual average values of λ and y are even higher. Equivalently, the *no-bubble hypothesis* is rejected in this case.

Remark 1. It is shown in the proof of the proposition that the $o_p(1)$-term in (15), w_N, satisfies the following bound $\mathbb{P}(|w_N| > q) \leq 2e^{-\frac{N}{2\bar{\sigma}^2}q^2 \ln(q\sqrt{2\pi})^2}$. This decreases sufficiently fast to ensure almost sure convergence, $w_N \rightarrow_{a.s.} 0$.

The lower bounds (16,17) can be used to verify that the crash risk *is* reasonably low, so that there is no bubble, i.e., to rule out type II errors. The bounds are especially useful when the average yield is known to be low, i.e., when $\bar{y}$ is close to zero. One such case arises when the yield is actually observed (for example, for stocks), and a total return process (including dividends) can be defined. The total return process, which is defined by $\frac{P_{(n+1)\Delta t} - P_{n\Delta t}}{P_{n\Delta t}} + y_n \Delta t$ in this case, then has the trivial bound $\bar{y} = 0$.

If the average yield may be high, then it will be difficult to distinguish dynamics where both average crash risk and average yield are high (and there is a bubble) from those where they are both low (and there is no bubble). The estimated variable Q^N, which can be both positive and negative, measures how much the estimated average crash risk is "downgraded" by high random realizations being estimated to occur exactly when volatility is high. If Q^N is high, there is a significant such "downgrading," and if the actual random realization differs from that estimated, the actual average crash risk $\bar{\lambda}_{N\Delta t}$ may be significantly higher than the estimated, λ^N. We therefore define

$$\check{L} = e^{-(\lambda^N + y^N + \bar{y} + Q_N)T},$$

which excludes the "downgrading," and therefore provides a lower bound on the survival probability consistent with observations and (16). Compare this with the estimate which includes the "downgrading," $\hat{L} = e^{-\lambda^N T}$.

2.3   An instructive example

An instructive example is given in Figure 1. Here, we assume only three return observations, with realizations $\mu_0 = 0.165$, $\mu_1 = 0.300$, $\mu_2 = 1.0698$. Assume that the expected return in each period is $u = 0.2$, and that the volatility is $\sigma_0 = 0.2$, $\sigma_1 = 1$, and $\sigma_2 = 0.4$.

As stated by (10), the random realizations of the ξ_m's in these three observations are assumed to be $G_1 = \Phi^{-1}(1/4) \approx -0.675$, $G_2 = \Phi^{-1}(1/2) \approx 0$, and $G_3 = \Phi^{-1}(3/4) \approx 0.675$. If we knew in which order these realizations occurred, we could back out λ_n and y_n. But, we do not know the

order. Indeed, there are six different possible permutations.[5] The realization of λ_t and y_t for each of these permutations are shown in panels 3-8 of the figure. Blue bars represent λ's and green bars y's. Panels 1 and 2 show the actual return realizations.

The sum of the λ's then lead to the survival probability $L = e^{-(\lambda_1 + \lambda_2 + \lambda_3)}$. We see that the "worst-case scenario" for the test, in the sense of the highest implied survival probability and thereby the most consistent dynamics with no bubbles, occurs in panel 3, which represents the permutation $(1,2,3)$. The survival probability under this scenario is $L \approx 44.9\%$ so if we set the threshold for identifying a bubble at a survival probability above 5%, we can then conclude that the return realizations are consistent with no bubble in this example.

The number of possible permutations is only 6 in this example with three observations, but increases quickly as the number of observations grows. The viability of our method relies on the possibility of solving the optimization problem in polynomial time, using the Hungarian algorithm. Indeed, we have verified that the method works well on a laptop for simulated problems with up to 10,000 observations, so we can conclude that the method works for up to 40 years of daily observations, and can be used at even higher frequencies over shorter time periods (or on a more powerful computer).

2.4 Variable discount rate CVP

Under the base specification, we have assumed that the risk adjusted discount rate is constant over time. The CVP can be extended to include assets for which the discount rate varies over time, also under the base specification with idiosyncratic risk. In continuous time, this corresponds to the specification

$$\frac{dV_s}{V_s} = (r_s + \lambda_s - y_s)ds + \sigma_s dW_s - dJ_s, \tag{18}$$

with the following average discount rate,

$$\bar{r}_t = \frac{1}{t}\int_0^t r_s ds.$$

This is therefore a *time varying discount rate specififcation* with idiosyncratic risk.

For the discrete CVP with variable rates, we assume that the average risk adjusted discount rate during the observation period is known, u, but that the per period discount rate may deviate from the sample mean,

$$u = \frac{1}{N}u_n. \tag{19}$$

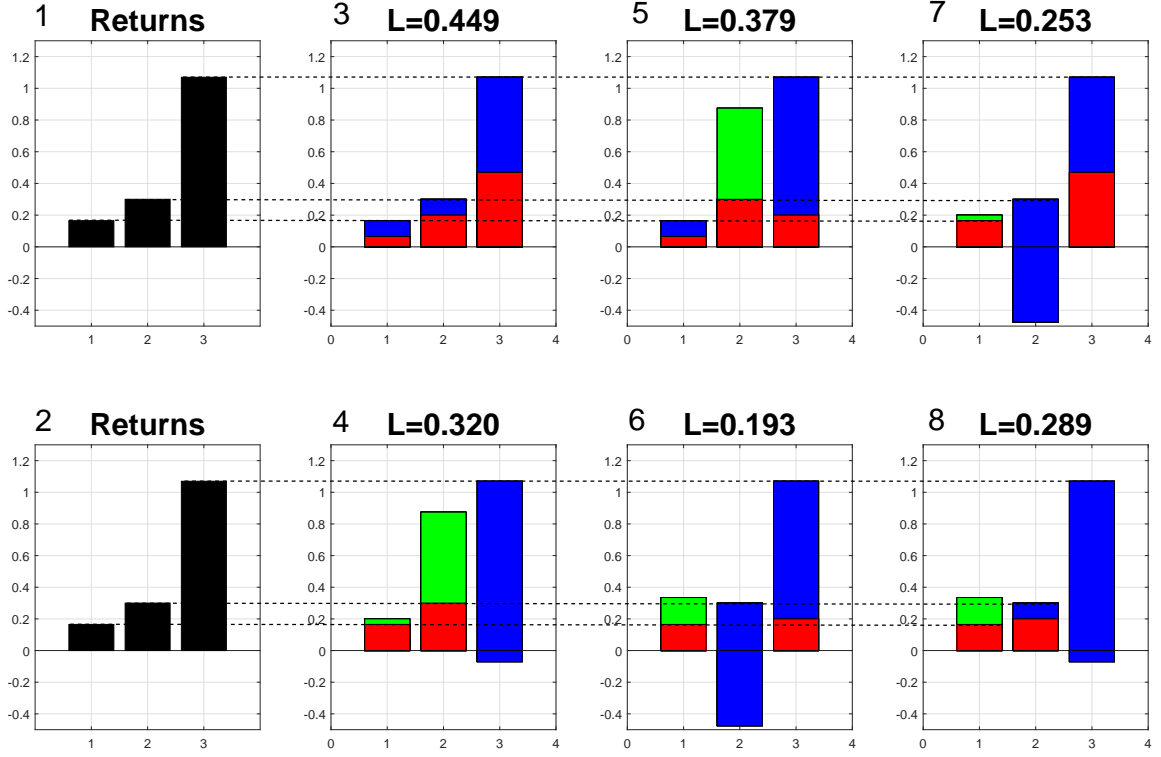[5]These are (1,2,3), (1,3,2), (2,1,3), (2,3,1), (3,1,2), and (3,2,1).

Figure 1: **An instructive example: Panels 1 and 2 show realized returns over three periods (and are identical). Panels 3-8 show the inferred λ_n's (blue bars) and $y'_n s$ (green bars) for the 6 possible permutations of G_1, G_2, and G_3. Panel 3 has the highest implied survival probability of** 44.9%**.**

Defining, $u_n^e = u_n - u$, it then follows that (9) is replaced in this formulation of the CVP, which assumes variable discount rates, by

$$\mu_n = u + u_n^e + \lambda_n - y_n + \sigma_n \xi_n, \tag{20}$$

and the variable CVP (V-CVP) is then:

Definition 3 (Variable CVP)**.** *Consider the observed processes μ_n and σ_n, $n = 1, 2, \ldots, N$, and the consistency set $\Gamma \overset{\text{def}}{=} [\underline{u}, \bar{u}] \times [0, \bar{\lambda}] \times [0, \bar{y}]$, where u defines the average discount rate, as in (19). These observations are said to be* consistent with fundamental values *if there exists a triplet $(u, \lambda, y) \in \Gamma$, sequences ξ_n and μ_n^e, and nonnegative sequencse λ_n and y_n, $n = 0, \ldots, N - 1$, such that*

1. $\sum_n u_n^e = 0$,

2. $\mu_n = u + u_n^e + \lambda_n - y_n + \sigma_n \xi_n$, $n = 0, \ldots, N - 1$,

3. $\lambda = \frac{1}{N} \sum_n \lambda_n$, and $y = \frac{1}{N} \sum_n y_n$,

4. *The empirical distribution function associated with $\{\xi_n\}_n$, F_ξ, is approximately that of a standard normal distribution, Φ: $||F_\xi - \Phi||_\infty < \epsilon(N)$, for some function $\epsilon(N) \to_{N\to\infty} 0$.*

By inspection, it follows that the solutions $\{\lambda_n\}_n$, $\{y_n\}_n$, to $CVP(u, 1/2)$ can be used to generate all solutions $\{u_n^e\}_n$, $\{\lambda_n^V\}_n$, $\{y_n^V\}_n$, to V-CVP. Specifically, the sequences $\{u_n^e\}_n$ such that $\sum_n u_n^e = 0$, and associated sequences

$$
\begin{aligned}
\lambda_n^V &= \lambda_n + u_n^e \times 1_{u_n^e < 0} \geq 0, \\
y_n^V &= y_n - u_n^e \times 1_{u_n^e > 0} \geq 0,
\end{aligned}
$$

define the solutions to V-CVP. In other words, variations in the discount rate can be used to "move" density between the estimated λ and y in V-CVP. Consequently, given $u \in [\underline{u}, \overline{u}]$, the bounds $\lambda \in [0, \overline{\lambda}]$, and $y \in [0, \overline{y}]$ are for V-CVP replaced by:

$$
\lambda - y \leq \overline{\lambda}, \tag{21}
$$

$$
y - \lambda \leq \overline{y}, \tag{22}
$$

where λ and y are the solutions to CVP. If such solutions to CVP can be found that satisfy (21,22), then a solution to V-CVP with parameters in the consistency set exists.

2.5 Comparison with Explosive Bubble tests

It is instructive to compare our approach with the SADF test, see Phillips et al. (2011) and Phillips et al. (2015b). That method tests for the presence of so-called *explosive bubbles* by studying the conjectured relationship

$$
p_{t+\Delta t} = \kappa + \nu p_t + \epsilon_t. \tag{23}
$$

Here, $p_t = \ln(P_t)$ represent log-prices. The authors define an explosive bubble to be present if $\nu > 1$, i.e., if the test finds a root with modulus higher than one.

This test for explosive bubbles is different from our fundamental value pricing test. Under the hypothesis of fundamental value pricing, $P_t = V_t$, and Ito's lemma leads to the following dynamic for p_t, while $t < \tau$:

$$
dp = d\ln(V) = \frac{dV}{V} - \frac{1}{2}\left(\frac{dV}{V}\right)^2.
$$

This, in turn, leads to

$$E[dp] = \left(r + \lambda_t - y_t - \frac{\sigma_t^2}{2} \right) dt.$$

Now, if $\lambda_t \sim \alpha p_t$, $\alpha > 0$, in some region of prices, i.e., if λ_t is increasing in log-prices in that region, we would expect the test to find:

$$E[\Delta p_t] = E[p_{t+\Delta t}] - p_t \sim \left(r - y_t - \frac{\sigma_t^2}{2} \right) \Delta t + \alpha \Delta t \, p_t,$$

which would suggest the presence of an explosive bubble in periods of price run-ups, even though the price of the asset reflects fundamental values, implying that there is no bubble present according to our terminology.

We conclude that for nontraditional assets it may be difficult to use explosive bubble tests to draw inferences about the presence of bubbles as defined in this paper, in the sense of deviations between prices from fundamental values.

3 Tests

We first study the performance of the CVP test in simulations, and then apply the test to detect bubbles in some stocks during the Dotcom boom, and to cryptocurrencies in recent periods.

3.1 Simulations

We run the CVP algorithm on a test bench of six simulated benchmark problems with 500 weekly returns (approximately 10 years in total). Per assumption, the price and volatility sequences, $\{P_n\}_{n=0,\dots,499}$ and $\{\sigma_n\}_{n=0,\dots,499}$, are observed, whereas the crash risk and yield processes, $\{\lambda_n\}_n$ and $\{y_n\}_n$, are unobserved. The six benchmark problems are shown in Figure 2. For each problem $u = 0.004$ per week, corresponding to approximately $r = 0.2$ per year. Moreover, $\{\lambda_n\}_n$ and $\{y_n\}_n$ are random and i.i.d. in all benchmark problems except for problem 5. This makes these problems challenging for CVP, which chooses these estimated processes to minimize the implied likelihood of a bubble.

We set the critical survival probability at $L = 5\%$, corresponding to $\bar{\lambda} = \frac{-\ln(0.05)}{10} = 0.2996$ per year. If the implied survival probability from the estimate provided by CVP is lower than this threshold, we reject the no-bubble hypothesis. Similarly, we define the maximum consistent yield to be $\bar{y} = 0.3$ per year. Summary statistics, as well as the results of CVP and the SADF test in Phillips et al. (2015b) are shown in Table 1.

The first series has a survival probability of $L = 12.87\%$, and is therefore consistent with funda-

mental prices. The estimated survival probability is $\hat{L} = 34.63\%$, so the test correctly fails to reject the null hypothesis. We note that this estimate is significantly higher than the actual probability, which is unsurprising: the $\{\lambda_n\}_n$ (as well as the $\{y_n\}_n$) sequences are randomly generated in all the benchmark problems, and will therefore typically affect the survival probability much less than when chosen to minimize the probability. It is this conservativeness that makes the method robust.

Similarly, the null is not rejected for the benchmark problems 3 and 5, in line with both problems having survival probabilities above 5%. Problem 5 has a crash intensity λ_n that is convex in P_t over a specific price range, as seen in the bump of the λ sequence around $n = 400$. This makes log-prices behave as if there is a feedback loop in that area, conditioned on there being no crash.

Benchmark problem 2 has a much lower survival probability and the null is also rejected for this problem by CVP, implying a bubble. We note that the price path for this problem is more dramatically increasing than for benchmark problem 1, driven by the higher λ_n's. However, a dramatic price increase is not necessary for a bubble to be detected. Indeed, the price path for problem 4 is less dramatic than for problem 1, although problem 4 contains a bubble ($L = 0.29\%$), whereas problem 1 does not. The reason for problem 4's modest price path behavior is that the yield sequence, $\{y_n\}_n$, is also high, pulling down prices. Despite this offset, CVP rejects the no-bubble hypothesis for problem 4, and detects that both the average crash risk and average yield are high — $\hat{\lambda} = 0.3524$ and $\hat{y} = 0.2658$. Finally, the no-bubble hypothesis is also rejected for benchmark problem 6, which indeed also contains a bubble ($L = 0.13\%$). Note also that the lower bound on the survival probability, $\check{L}$ is higher than 5% for all three no-bubble economies, suggesting that one can robustly view these economies as no-bubble economies.

In contrast, the SADF statistic has a hard time to characterize these benchmark problems correctly, as seen in row 7 of Table 1. The critical value of rejecting the no-bubble hypothesis at the 5% level for these datasets is about 1.5. As suggested earlier, the SADF test detects a bubble in the feedback benchmark problem 5 ($SADF = 1.689$), although no deviation from fundamental values is present (the true survival probability is $L = 48.7\%$), most likely because of the positive relation between prices and crash risk. Also, the test strongly rejects the no-bubble hypothesis (at the 1% level, $SADF = 2.37$) for problem 1, which does not contain a bubble ($L = 12.87\%$) and, moreover, fails to detect bubbles for problems 2 and 4 ($L = 0.87\%$ and $L = 0.29\%$, respectively, for these two problems). We conclude that the challenges for the SADF test to classify whether fundamental value deviations are present are severe in our nontraditional asset setting.

To explore how efficient CVP is in detecting bubbles — defined by dynamics with actual survival probabilities of $L \leq 5\%$ — we simulate 1000 price paths with i.i.d. processes for λ_n and y_n, 500

Simulation	1	2	3	4	5	6
Bubble	**No**	**Yes**	**No**	**Yes**	**No**	**Yes**
$\bar{\sigma}$	0.3599	0.3513	0.3590	0.3486	0.3495	0.3573
λ	0.2050	0.4740	0.1975	0.5829	0.0720	0.6608
y	0.0360	0.0450	0.2000	0.5846	0	0.2932
L	**0.1287**	**0.0087**	**0.1388**	**0.0029**	**0.4870**	**0.0013**
SADF	2.37	0.830	-0.627	0.639	1.689	0.778
$\hat{\lambda}$	0.1103	0.3259	0.0387	0.3524	0.0519	0.3573
$\hat{y}$	0.0039	0.0017	0.0678	0.2658	0.0082	0.0742
$\check{L}$	**0.11895**	**0.00525**	**0.07078**	**0.00000**	**0.22247**	**0.00059**
$\hat{L}$	**0.3463**	**0.0435**	**0.6895**	**0.0338**	**0.6072**	**0.0322**

Table 1: **Consistency verification for simulated data (at $L = 5\%$ level). Benchmark problems in panels 1,3, and 5, are consistent with fundamental prices. Benchmark problems in panels 2, 4 and 6 not consistent, as shown in row 2. Rows 3-5 contain actual sample averages of σ_n, λ_n, and y_n, annualized. Row 6 contains actual survival probability. Row 7 contains the SADF statistic defined in Phillips et al. (2011). Rows 8-9 contain estimated crash risk process and yield from CVP, and row 10 the implied survival likelihood. The no-bubble null hypothesis is rejected when $\hat{L} < 5\%$. Per period discount rate $u = 0.004$ for all problems.**

weeks of observations for each path, assuming a known discount rate $r = 0.1$. For each path, $(\hat{\lambda}, \hat{y}) = CVP(r, 1/2)$ is calculated, leading to the implied survival probability $\hat{L} = e^{-\hat{\lambda}T}$. The cutoff threshold for λ, corresponding $L = 5\%$ is then $\lambda = 0.30$.

The results are shown in Figure 3. Out of the 1000 simulations, 613 are correctly classified as being consistent with fundamental value pricing, and 258 are correctly classified as being inconsistent. Of the 129 incorrectly classified price paths (12.9% of the total number of simulations), the vast majority are "type II errors," i.e., failure to reject the no-bubble hypothesis although the survival probability is less than 5%. These are the observations in the lower right quadrant of the figure. There are only 9 "type I error" classifications (corresponding to 0.9% of the sample), i.e., rejections of the no-bubble hypothesis even though the actual survival probability is higher than 5%. This disproportion represents the conservative nature of the method, which looks at all possible realizations of crash risk and yield that are consistent with the observed price path, and chooses the realizations that minimizes their averages.

3.2 Tests on stocks

We run our test on a set of traditional assets, namely stocks. During the so-called Dotcom boom, which lasted roughly from 1995 until early 2000, prices of Internet stocks and other related tech stocks

quickly increased, and then subsequently collapsed (the peak occurred in March 2000). Many have in hindsight viewed this as a bubble.[6]

An advantage of studying stocks is that their surplus is observed; it is the dividends the stock pays. We may therefore study total returns, including dividends, and set $\bar{y} = 0$ for the total return process. A challenge with studying the Dotcom boom is that many of the stocks involved were only publicly traded fpr a short period before the collapse, because their IPOs occurred in 1998 or 1999.

We pick a sample of eight stocks, four of which — Microsoft, IBM, Ericsson, and Cisco — were traditional tech stocks that were affected by the boom, and the other four — Yahoo, theGlobe.com, Garden.com, and Vignette Corporation — were firms with more recent IPOs. We also include two major stock indexes, S&P 500 and Nasdaq. We set the upper bound of the discount rate at $\bar{r} = 15\%$, a high number, but not unreasonable for an individual stock.

The results are shown in Table 2. We see that for none of the stocks is the presence of a bubble unambigously determined, in the sense of the survival probability $\hat{L} < 5\%$. The stocks that come closest to the threshold are Yahoo, with $\hat{L} = 0.0943$, and Cisco, with $\hat{L} = 0.1093$. For both these stock, the lower estimates, $\check{L}$, are well below the bubble threshold, so a bubble is not ruled out, whereas for the other stocks and the indexes, the lower bounds are also above the bounds, more strongly suggesting that a bubble was not present in either of these.

Note that the estimated average crash intensity is very high for Vignette Corporation, at $\lambda = 1.7640$. Our model sugggests that the market understood that the company was a risky investment, but still viewed it as worhwhile since, it would become very valuable in case a crash was avoided. But a crash was not avoided. Indeed, at its peak in 2000 Vignette Corporation was worth almost USD 10 Billion, while it was acquired for USD 320 million by Open Text Corporation in 2009. This corresponds to a collapse of close to 97% of the company's value.

We also study stocks and the market over a longer horizon. In Table 3, we show the estimated survival probabilities, based on total returns between 1990 and 2020, for the tech stocks from the test, as well as for Facebook, which after its IPO in 2012 has experienced strong growth. We also include the S&P 500 and Nasdaq indexes, as well as the CRSP Total Market return index. Over this longer period, and since these companies are mature, set the discount rate at $\bar{r} = 11\%$, which is about the long-term average market return per year.

Again, a bubble is not unambiguously suggested in this sample. The closest company to an unambiguous bubble is Cisco, followed by Microsoft. These two companies had very strong performances

---

[6]There is no consensus about the Dotcom boom being a bubble period. Pastor and Veronesi (2006) suggest that the valuation of Nasdaq could be explained by high uncertainty about the benefits of new technologies. This explanation is potentially in line with our model (the crash occurs if the technology does not work).

	MSFT	IBM	ERICY	CSCO	YHOO	TGLO	GDEN	VGNT	S&P 500	Nasdaq
Start date	Jan 95	Jan 95	Jan 95	Jan 95	Apr 96	Nov 98	Sep 99	Feb 99	Jan 95	Jan 95
$\hat{\lambda}$	0.2921	0.1687	0.3289	0.4444	0.6298	0.2919	0.3553	1.7640	0.0636	0.1319
$\hat{y}$	0.0116	0.0154	0.0511	0.0099	0.0439	0.8944	1.8729	0.0949	0.0107	0.0045
$\check{L}$	0.0991	0.1927	0.0503	0.0318	0.0060	0.1835	0.4367	0.0523	0.6371	0.4864
$\hat{L}$	0.2334	0.4317	0.1943	0.1093	0.0943	0.6982	0.8604	0.1773	0.6910	0.4648

Table 2: **Testing for bubbles during Dotcom boom. Included in the test are traditional tech stocks: Mircorosft, IBM, Ericsson, Cisco; Dot.com stocks: Yahoo, TheGlobe.com, Garden.com, Vignette Corporation; Indexes: S&P 500, Nasdaq. Tests based on weekly returns and conditional volatility estimated from daily returns in preceding two weeks.**

	MSFT	IBM	ERICY	CSCO	FB	S&P 500	Nasdaq	Market
Start date	Jan 90	Jan 90	Jan 90	Jan 90	May 12	Jan 90	Jan 90	Jan 90
$\hat{\lambda}$	0.0871	0.0296	0.0790	0.0962	0.1377	0.0418	0.0617	0.0449
$\hat{y}$	0.0252	0.0424	0.0701	0.0247	0.0594	0.0216	0.0050	0.0128
$\check{L}$	0.0064	0.1668	0.0061	0.0019	0.0841	0.4004	0.2778	0.3141
$\hat{L}$	0.0732	0.4107	0.0933	0.0564	0.3184	0.2855	0.1570	0.2490

Table 3: **Testing for bubbles 1990-2020. Included in the test are: Mircorosft, IBM, Ericsson, Cisco, Facebook; Indexes: S&P 500, Nasdaq, Total Market (CRSP). Tests based on weekly returns and conditional volatility estimated from daily returns in preceding two weeks.**

over the period. Of the remaining companies, Ericsson is the only one for which a bubble is not ruled out, i.e., for which it is not the case that $\check{L} \geq 5\%$. We have carried out several variations of these tests (not reported) with similar results, namely (i) that bubbles are in general not unambiguously indentified, in that it is typically the case that $\bar{L} \geq 0.05$; and (ii) they are often ruled out in that $\check{L} \geq 0.05$. For Ericsson, the lower bound is $\check{L} = 0.0061$, is well within the range of a bubble.

Interestingly, the average return on Ericsson stock was not high during the period (CAGR of 5.89% per year). The reason it is hard to rule out a bubble for Ericsson is that its growth during the Dotcom boom was quite dramatic, after which it fell back. Indeed, after the peak on March 2, 2000, Ericsson's cumulative total return has been -83.2%. This is another example of what we saw earlier in Section 3.1, that our test does not simply rely on total returns during the period.

Similar results as those provided here are obtained under several variations (not reported): for major indexes and several major stocks over even longer time periods (50 years), varying the estimation window for conditional volatility between 5 days and a month, and varying the discount rate between 10% and 20%.

3.3 Tests on cryptocurrencies

We identify the set of cryptocurrencies with a market value of \$1 Billion or higher (as of May 11, 2022). In contrast to stocks, we do not have as strong a view about what constitutes a reasonable range of discount rates for cryptocurrencies. We choose to be really conservative, and view any annual discount rate below 50% per year as reasonable, i.e., we view $r \in [0, 0.5]$ as the reasonable range of discount rates. We run the CVP-test on these 54 cryptocurrencies with market values above \$1 Billion, under the hypothesis that $r = 0.25$, as well as $r = 0.5$. Our sample ends on May 9, 2022. The results are shown in Table 4. As in the simulations, we use weekly observations for the price series. The instantaneous volatility is calculated using a 7-day window of (non-overlapping) daily observations. Three cryptocurrencies are unambiguously identified as containing bubbles: Ethereum (ETH),[7] Solana (SOL), and Stellar (XLM). Figure 4 shows prices of Ethereum and Stellar, side by side with two cryptocurrencies that are *not* unambiguously identified as containing bubbles, Bitcoin (BTC), and Dogecoin (DOGE).

We also run the test using the Sharpe ratio specification, with $\rho = 1$, i.e., assuming only market risk in the nontraditional asset. The results, shown in Table 5, reaffirm our previous results. With a market Sharpe ratio of 0.4 (per year), Ethereum, Solana, and Stellar are again identified as containing bubbles. When the Sharpe ratio is increased to the very high level of 0.7, Solana no longer makes the list whereas Ethereum (Classic) and Stellar remain in the bubble region.

We note that visually, the price behavior of these four cryptocurrencies look quite similar. Also, although only three cryptocurrencies unambiguously are identified as containing bubbles (by $\hat{L}$), about half of the cryptocurrencies are identified as *possibly* containing bubbles (by $\check{L}$).

We further study four major cryptocurrencies: Bitcoin, Ethereum, Dogecoin, and Stellar coin. We solve $CVP(r, 1/2)$ for equidistant choices of r inside and outside of the range, $r \in [0, 1]$, and calculate the implied average crash risk ($\hat{\lambda}$), yield ($\hat{y}$), and survival probability ($\hat{L}$) for each of these discount rates. As in the simulations, we set $\hat{L} = 5\%$ as the critical value for rejecting the no-bubble hypothesis. We do not have a strong view of what is an appropriate upper threshold for y, and therefore choose a fairly high value, $\bar{y} = 0.3$ per year.

The result for Bitcoin is shown in Figure 5. As seen from the figure, the threshold for Bitcoin lies at about $r = 0.18$, so we cannot conclude that a bubble is present. The same test for Ethereum Classic is shown in Figure 6. Here, we see that up to a significantly higher discount rate, $r > 0.72$, the no-bubble hypothesis is rejected. Figures 7 shows the same CVP tests for Dogecoin, for which

---

[7]Ethereum Classic (ETC) has a very similar behavior as Ethereum (ETH), and we therefore count them as the same observation.

the no-bubble hypothesis is not even rejected at $r = 0$. For Stellar, the no-bubble hypothesis is unambiguously rejected even at the very high risk adjusted discount rate $r = 1$.

4   Conclusions

We have presented a new method to test for the presence of bubbles, especially suitable for assets where the use value is not easy to determine. We do not find that there is a bubble in Bitcoin. From being a computer science curiosity it has has seen wide adoption and in some parts of the world, even retail investors are using it as a store of value. Although Bitcoin is too volatile to be a successful means of payment, it has increasingly become an attractive investment for those who want exposure to cryptocurrencies. In as much as the dollar only has value because all accept it has value so Bitcoin has use value because it is accepted as such. By contrast, Ethereum does have a concrete use value – payment for executing code on the blockchain. However, as competing chains are brought online, and Ethereum moves to more efficient processing, the use value will plausibly decline over time. As it is not the focal cryptocurrency asset that investors hold in their portfolio, the price could admit a bubble.

Name	No. obs.	r = 0.25				r = 0.5			
		$\hat{\lambda}$	$\hat{y}$	$\hat{L}$	$\check{L}$	$\hat{\lambda}$	$\hat{y}$	$\hat{L}$	$\check{L}$
AAVE	921	0.0228	0.0034	0.0519	0.0000	0.0217	0.0035	0.0593	0.0000
ADA	1593	0.0055	0.0032	0.2897	0.0233	0.0049	0.0043	0.3271	0.0307
ALGO	241	0.0011	0.0238	0.9638	0.5566	0.0011	0.0261	0.9651	0.5376
APE	54	0.0922	0.0141	0.5750	0.4394	0.0899	0.0153	0.5832	0.4425
ATOM	148	0.0097	0.0161	0.8234	0.5537	0.0084	0.0183	0.8452	0.5439
AVAX	494	0.0405	0.0019	0.0611	0.0052	0.0393	0.0014	0.0663	0.0071
AXS	554	0.0351	0.0019	0.0646	0.0001	0.0333	0.0022	0.0747	0.0002
BCH	1744	0.0030	0.0028	0.4795	0.0092	0.0024	0.0043	0.5505	0.0104
BNB	1645	0.0100	0.0005	0.0960	0.0003	0.0082	0.0006	0.1457	0.0007
BSV	1271	0.0006	0.0072	0.8909	0.0121	0.0007	0.0089	0.8894	0.0126
BTC	3053	0.0058	0.0002	0.0806	0.0045	0.0045	0.0005	0.1416	0.0167
BTCB	382	0.0071	0.0094	0.6878	0.3944	0.0067	0.0105	0.6993	0.4206
BTT	107	0.0011	0.0180	0.9841	0.7052	0.0009	0.0212	0.9876	0.6760
CAKE	241	0.0031	0.0179	0.9015	0.7954	0.0034	0.0192	0.8953	0.8203
CRO	1218	0.0166	0.0023	0.0567	0.0005	0.0154	0.0031	0.0696	0.0006
DAI	1558	0.0000	0.0021	0.9944	1.0113	0.0000	0.0041	0.9948	0.9192
DOGE	1804	0.0083	0.0063	0.1199	0.0000	0.0080	0.0079	0.1290	0.0000
DOT	458	0.0133	0.0061	0.4270	0.3643	0.0113	0.0070	0.4840	0.4049
EGLD	241	0.0109	0.0170	0.6987	0.5422	0.0092	0.0188	0.7381	0.5406
EOS	1776	0.0038	0.0021	0.3824	0.0128	0.0032	0.0034	0.4454	0.0165
ETC	2115	0.0124	0.0036	**0.0240**	0.0001	0.0114	0.0049	**0.0325**	0.0001
ETH	2254	0.0120	0.0004	**0.0214**	0.0002	0.0104	0.0007	**0.0356**	0.0005
FIL	1560	0.0020	0.0047	0.6407	0.0263	0.0019	0.0060	0.6545	0.0324
FLOW	207	0.0116	0.0265	0.7224	0.5517	0.0107	0.0286	0.7401	0.5411
FTT	241	0.0071	0.0129	0.7922	0.7014	0.0066	0.0147	0.8054	0.7017
HBAR	945	0.0051	0.0037	0.5040	0.0111	0.0043	0.0051	0.5599	0.0123
HNT	385	0.0094	0.0090	0.6034	0.2386	0.0087	0.0105	0.6256	0.2454
HT	1355	0.0037	0.0011	0.4897	0.0595	0.0030	0.0021	0.5607	0.0794
ICP	365	0.0006	0.0371	0.9716	0.2561	0.0011	0.0387	0.9466	0.2596
KCS	1576	0.0070	0.0047	0.2071	0.0055	0.0065	0.0060	0.2333	0.0069
KLAY	241	0.0049	0.0169	0.8509	0.6170	0.0042	0.0194	0.8693	0.5868
LEO	1051	0.0021	0.0008	0.7279	0.3210	0.0013	0.0017	0.8231	0.4088
LINK	1561	0.0118	0.0006	0.0720	0.0025	0.0098	0.0009	0.1130	0.0048
LTC	2088	0.0052	0.0020	0.2139	0.0003	0.0044	0.0030	0.2731	0.0005
LUNA	241	0.0301	0.0012	0.3700	0.2422	0.0280	0.0011	0.3974	0.2743
MANA	1561	0.0038	0.0012	0.4274	0.0028	0.0027	0.0023	0.5470	0.0040
MATIC	1051	0.0104	0.0019	0.2112	0.0002	0.0088	0.0026	0.2688	0.0003
MKR	1540	0.0019	0.0033	0.6607	0.0377	0.0016	0.0048	0.7076	0.0414
NEAR	241	0.0123	0.0066	0.6659	0.2930	0.0104	0.0079	0.7090	0.3031
RUNE	357	0.0141	0.0122	0.4946	0.2024	0.0127	0.0138	0.5299	0.2075
SAND	159	0.0059	0.0369	0.8840	0.4225	0.0056	0.0388	0.8885	0.4191
SHIB	366	0.0449	0.0187	0.1012	0.0075	0.0446	0.0207	0.1030	0.0074
SOL	639	0.0374	0.0005	**0.0347**	0.0024	0.0348	0.0008	**0.0435**	0.0031
THETA	1537	0.0070	0.0005	0.2195	0.0024	0.0053	0.0008	0.3125	0.0046
TRX	1641	0.0118	0.0013	0.0644	0.0000	0.0108	0.0021	0.0801	0.0000
UNI	241	0.0015	0.0228	0.9516	0.6782	0.0008	0.0255	0.9745	0.6368
USDT	1853	0.0000	0.0023	0.9977	0.8860	0.0000	0.0050	0.9981	0.5652
VET	1674	0.0054	0.0026	0.2798	0.0005	0.0047	0.0034	0.3247	0.0008
WBTC	241	0.0066	0.0092	0.8050	0.6753	0.0054	0.0111	0.8376	0.6693
XLM	1906	0.0186	0.0055	**0.0064**	0.0000	0.0179	0.0069	**0.0078**	0.0000
XMR	2660	0.0077	0.0006	0.0531	0.0000	0.0061	0.0008	0.0979	0.0000
XRP	2667	0.0053	0.0055	0.1353	0.0000	0.0049	0.0069	0.1574	0.0000
XTZ	1561	0.0036	0.0035	0.4514	0.0294	0.0032	0.0045	0.4938	0.0407
ZEC	2022	0.0047	0.0037	0.2613	0.0200	0.0041	0.0048	0.3096	0.0286

Table 4: **Tests for cryptocurrencies with market value above USD\$1 Billion.**

Name	No. obs.	$S = 0.4$				$S = 0.7$			
		$\hat{\lambda}$	$\hat{y}$	$\hat{L}$	$\check{L}$	$\hat{\lambda}$	$\hat{y}$	$\hat{L}$	$\check{L}$
AAVE	921	0.0340	0.0033	**0.0120**	0.0000	0.0128	0.0037	0.1893	0.0000
ADA	1593	0.0050	0.0039	0.3247	0.0403	0.0041	0.0059	0.3957	0.0653
ALGO	241	0.0006	0.0254	0.9811	0.5584	0.0006	0.0295	0.9800	0.5133
APE	54	0.0856	0.0164	0.5984	0.4512	0.0826	0.0193	0.6091	0.4619
ATOM	148	0.0076	0.0186	0.8582	0.5490	0.0064	0.0224	0.8792	0.5379
AVAX	494	0.0379	0.0017	0.0730	0.0087	0.0340	0.0024	0.0958	0.0142
AXS	554	0.0298	0.0025	0.0981	0.0003	0.0244	0.0042	0.1494	0.0005
BCH	1744	0.0027	0.0035	0.5181	0.0203	0.0018	0.0058	0.6361	0.0335
BNB	1645	0.0091	0.0004	0.1195	0.0008	0.0071	0.0005	0.1919	0.0031
BSV	1271	0.0006	0.0079	0.9057	0.0213	0.0003	0.0101	0.9405	0.0313
BTC	3053	0.0059	0.0002	0.0766	0.0086	0.0048	0.0003	0.1223	0.0479
BTCB	382	0.0066	0.0107	0.7037	0.4040	0.0062	0.0122	0.7192	0.4635
BTT	107	0.0009	0.0182	0.9870	0.7051	0.0006	0.0212	0.9923	0.6796
CAKE	241	0.0032	0.0184	0.9003	0.8422	0.0025	0.0217	0.9206	0.8074
CRO	1218	0.0156	0.0027	0.0677	0.0007	0.0141	0.0035	0.0873	0.0014
DAI	1558	0.0004	0.0007	0.9069	0.9307	0.0004	0.0008	0.9165	1.0262
DOGE	1804	0.0079	0.0063	0.1335	0.0001	0.0070	0.0083	0.1667	0.0018
DOT	458	0.0112	0.0075	0.4870	0.4089	0.0086	0.0099	0.5753	0.4589
EGLD	241	0.0092	0.0191	0.7380	0.5406	0.0076	0.0225	0.7770	0.5276
EOS	1776	0.0033	0.0028	0.4309	0.0320	0.0026	0.0044	0.5245	0.0785
ETC	2115	0.0116	0.0043	**0.0306**	0.0001	0.0103	0.0062	**0.0456**	0.0003
ETH	2254	0.0112	0.0005	**0.0277**	0.0006	0.0092	0.0010	0.0528	0.0024
FIL	1560	0.0020	0.0050	0.6365	0.0508	0.0016	0.0070	0.7061	0.0778
FLOW	207	0.0110	0.0278	0.7359	0.5499	0.0102	0.0317	0.7521	0.5092
FTT	241	0.0069	0.0139	0.7956	0.6986	0.0064	0.0160	0.8105	0.7004
HBAR	945	0.0044	0.0047	0.5534	0.0165	0.0039	0.0073	0.5921	0.0207
HNT	385	0.0080	0.0105	0.6476	0.2669	0.0060	0.0144	0.7219	0.2528
HT	1355	0.0039	0.0010	0.4775	0.0884	0.0028	0.0019	0.5825	0.1425
ICP	365	0.0009	0.0396	0.9566	0.2658	0.0004	0.0446	0.9789	0.2327
KCS	1576	0.0064	0.0053	0.2376	0.0099	0.0056	0.0070	0.2867	0.0175
KLAY	241	0.0046	0.0173	0.8586	0.6251	0.0043	0.0191	0.8690	0.6345
LEO	1051	0.0029	0.0005	0.6457	0.3257	0.0023	0.0007	0.7117	0.4570
LINK	1561	0.0097	0.0009	0.1172	0.0070	0.0070	0.0017	0.2129	0.0226
LTC	2088	0.0045	0.0024	0.2620	0.0007	0.0036	0.0037	0.3431	0.0017
LUNA	241	0.0263	0.0015	0.4195	0.2916	0.0232	0.0035	0.4652	0.3279
MANA	1561	0.0030	0.0020	0.5156	0.0070	0.0025	0.0034	0.5792	0.0192
MATIC	1051	0.0084	0.0028	0.2876	0.0005	0.0070	0.0041	0.3530	0.0012
MKR	1540	0.0017	0.0041	0.6834	0.0650	0.0014	0.0062	0.7371	0.1001
NEAR	241	0.0095	0.0089	0.7306	0.3182	0.0062	0.0110	0.8148	0.3650
RUNE	357	0.0125	0.0147	0.5364	0.2343	0.0101	0.0192	0.6031	0.2342
SAND	159	0.0051	0.0386	0.8984	0.4260	0.0037	0.0420	0.9252	0.4191
SHIB	366	0.0436	0.0205	0.1085	0.0089	0.0422	0.0230	0.1161	0.0103
SOL	639	0.0337	0.0006	**0.0484**	0.0045	0.0291	0.0009	0.0731	0.0090
THETA	1537	0.0052	0.0010	0.3226	0.0066	0.0035	0.0024	0.4693	0.0173
TRX	1641	0.0108	0.0018	0.0806	0.0001	0.0095	0.0029	0.1093	0.0002
UNI	241	0.0007	0.0248	0.9758	0.6645	0.0003	0.0289	0.9894	0.6096
USDT	1853	0.0001	0.0002	0.9823	1.0325	0.0001	0.0002	0.9842	1.1053
VET	1674	0.0044	0.0034	0.3470	0.0015	0.0033	0.0052	0.4515	0.0037
WBTC	241	0.0065	0.0095	0.8062	0.6779	0.0056	0.0111	0.8304	0.6846
XLM	1906	0.0174	0.0064	**0.0090**	0.0000	0.0160	0.0084	**0.0133**	0.0000
XMR	2660	0.0065	0.0007	0.0842	0.0001	0.0046	0.0009	0.1755	0.0022
XRP	2667	0.0050	0.0063	0.1517	0.0000	0.0046	0.0080	0.1747	0.0000
XTZ	1561	0.0032	0.0042	0.4941	0.0563	0.0024	0.0063	0.5813	0.0899
ZEC	2022	0.0040	0.0044	0.3166	0.0509	0.0033	0.0064	0.3864	0.1056

Table 5: **Test for cryptocurrencies with market value above USD$1 Billion. Sharpe ratio specification.**

A Proofs

Proof of Proposition 1: Defining the discrete norms $\|x\|_\infty = \max_{n=0,1\ldots,N-1} |x_n|$, and $\|x\|_1 = \frac{1}{N}\sum_{n=0}^{N-1} |x_n|$, it follows that the CVP algorithm solves

$$\min_{\hat{\lambda},\hat{y}} \; \alpha\|\hat{\lambda}\|_1 + (1-\alpha)\|\hat{y}\|_1, \;\; \text{s.t.} \tag{24}$$

$$\|G_\Pi - \hat{x}\|_\infty = 0, \tag{25}$$

where

$$\hat{x}_n = \frac{q_n - \hat{\lambda}_n + \hat{y}_n}{\sigma_n}, \tag{26}$$

and the permutation operator Π^{-1} provides the sorting of $\hat{x}_n$, i.e., $\hat{x}_{\Pi^{-1}(0)} < \hat{x}_{\Pi^{-1}(1)} < \cdots < \hat{x}_{\Pi^{-1}(N-1)}$.

The following lemma shows almost sure convergence of the norms of the solution to (24-26) and the equivalent problem based on the actual realizations of $\{\xi_n\}_n$.

Lemma 1. *Consider observations $\{\sigma_n\}_n$, and $\{q_n\}_n$, where*

$$q_n = \lambda_n - y_n + \sigma_n \xi_n, \qquad n = 0,\ldots,N-1,$$

and $\xi_n \sim N(0,1)$ are i.i.d. Define the permutation operator Π_0, such that $\xi_{\Pi_0^{-1}(0)} < \xi_{\Pi_0^{-1}(1)} < \cdots < \xi_{\Pi_0^{-1}(N-1)}$, and the approximate realizations of ξ_n:

$$\hat{\xi}_n = \Phi^{-1}\left(\frac{1 + \Pi_0(n)}{1+N}\right) = G_{\Pi_0(n)}. \tag{27}$$

Then, the solutions to the two problems:

$$E^a(N) = \min_{\hat{\lambda}^a,\hat{y}^a,\Pi_a} \; \alpha\|\hat{\lambda}^a\|_1 + (1-\alpha)\|\hat{y}^a\|_1, \;\; s.t. \tag{28}$$

$$\|\hat{\xi}_{\Pi_a} - \hat{x}^a\|_\infty = 0, \tag{29}$$

$$\hat{x}_n^a = \frac{q_n - \hat{\lambda}_n^a + \hat{y}_n^a}{\sigma_n}, \tag{30}$$

and

$$E^b(N) = \min_{\hat{\lambda}^b,\hat{y}^b,\Pi_b} \; \alpha\|\hat{\lambda}^b\|_1 + (1-\alpha)\|\hat{y}^b\|_1, \;\; s.t. \tag{31}$$

$$\|\xi_{\Pi_b} - \hat{x}^b\|_\infty = 0, \tag{32}$$

$$\hat{x}_n^b = \frac{q_n - \hat{\lambda}_n^b + \hat{y}_n^b}{\sigma_n}, \tag{33}$$

converge to the same value almost surely,

$$\lim_{N\to\infty} E^a(N) - E^b(N) = 0, \; a.s.$$

27

Note that the a-problem is identical to the CVP problem (24-26). It assumes that the random realizations of $\{\xi\}_n$ are exactly those of the G-function, i.e., of the inverse normal distribution evaluated at equidistant points, whereas the b-problem is based on the actual realizations of the ξ's, which are random. In this sense, the a-problem provides an approximate solution to the b-problem.

Since the actual $\{\xi\}_n$ realizations are unobservable the b-problem is not solvable by the econometrician. The a-problem is solvable, however, and since the lemma implies that the two converge to the same estimates, we can draw inferences about the solution to the (actual) b-problem by analyzing the (approximate) a-problem.

$Proof\ of\ Lemma\ 1$: Choose a confidence level β arbitrarily close to 100%, and a strictly positive ϵ arbitrarily close to 0. By the Glivenko-Cantelli theorem, the empirical distribution function F of $\{\xi_n\}_n$ is close to the normal distribution: $\mathbb{P}(\|F - \Phi\|_\infty < \epsilon) \geq \beta$ for sufficiently large N, where the infinity norm is defined for functions on the real line: $f : \mathbb{R} \to \mathbb{R}$,

$$\|f\|_\infty = \sup_x |f(x)|.$$

Now, consider the solution to the b-problem, with associated permutation operator Π_b, so that $\xi_{\Pi_b^{-1}(n)}$ is increasing in n. Then, by the Glivenko-Cantelli theorem it follows that

$$\mathbb{P}\left(\left|\Phi(\xi_{\Pi_b^{-1}(n)}) - \frac{n}{N}\right| \leq \epsilon, \ \forall n\right) \geq \beta. \tag{34}$$

Indeed, it follows from the Doretzky-Kiefer-Wolfowitz-Massart (DKW) inequality, see Massart (1990), that

$$\mathbb{P}\left(\exists n \in \{0, 2, \ldots, N-1\} : \left|\Phi(\xi_{\Pi_b^{-1}(n)}) - \frac{n+1}{N+1}\right| \geq \epsilon\right) \leq 2e^{-2N\epsilon^2},$$

so we can choose

$$\beta(\epsilon; N) = 1 - 2e^{-2N\epsilon^2}$$

in (34).

Focusing on such a β-probability event, such that $\left|\Phi(\xi_{\Pi_b^{-1}(n)}) - \frac{n}{N}\right| < \epsilon$ for all n, and defining $\epsilon_n = \Phi(x_{\Pi_b^{-1}(n)}) - \frac{n+1}{N+1}$, and

$$\hat{\lambda}^a_{\Pi_b^{-1}(n)} = \hat{\lambda}^b_{\Pi_b^{-1}(n)} + \sigma_n\left(\Phi^{-1}\left(\frac{n+1}{N+1} + \epsilon_n\right) - \Phi^{-1}\left(\frac{n+1}{N+1}\right)\right) \times 1_{\epsilon_n > 0}, \tag{35}$$

$$\hat{y}^a_{\Pi_b^{-1}(n)} = \hat{y}^b_{\Pi_b^{-1}(n)} + \sigma_n\left(\Phi^{-1}\left(\frac{n+1}{N+1}\right) - \Phi^{-1}\left(\frac{n+1}{N+1} + \epsilon_n\right)\right) \times 1_{\epsilon_n < 0}, \tag{36}$$

where $\hat{\lambda}^b$ and $\hat{y}^b$ are the solutions to the b-problem; and then finally defining

$$\hat{x}^a_n = \frac{q_n - \hat{\lambda}^a_n + \hat{y}^a_n}{\sigma_n},$$

it follows that $\|G_{\Pi_b} - \hat{x}^a\|_\infty = 0$. In other words, $(\Pi_b, \{\hat{\lambda}^a_n\}_n, \{\hat{y}^a_n\}_n)$ defines a candidate solution to the a-problem, which is based on the same permutation operator as the one that solves the b-problem.

Thus,
$$E^a \leq \alpha \|\hat{\lambda}^a\|_1 + (1-\alpha)\|\hat{y}^a\|_1, \tag{37}$$

since the actual solution to the a-problem cannot be larger than this candidate solution. Note that $|\epsilon_n| \leq \epsilon$, $\forall n$, for such a β-probability event.

For the solution to the b-problem and candidate solution to the a-problem, with the associated β event and ϵ, we now use (35) to write

$$
\begin{aligned}
\|\hat{\lambda}^a - \hat{\lambda}^b\|_1 &\leq \frac{\bar{\sigma}}{N} \sum_n \left| \Phi^{-1}\left(\frac{n+1}{N+1} + \epsilon\right) - \Phi^{-1}\left(\frac{n+1}{N+1}\right) \right| \\
&\leq 2\bar{\sigma} \int_{1/2}^{1-\epsilon} \Phi^{-1}(s+\epsilon) - \Phi^{-1}(s)ds + C\frac{1}{N} \\
&= 2\bar{\sigma} \left(-\int_{1/2}^{1/2+\epsilon} \Phi^{-1}(s)ds + \int_{1-\epsilon}^{1} \Phi^{-1}(s)ds \right) \\
&\leq 2\bar{\sigma} R(\epsilon) + C\frac{1}{N},
\end{aligned}
$$

where
$$R(\epsilon) = \int_{1-\epsilon}^{1} \Phi^{-1}(s)ds, \qquad \epsilon \in [0, 1/2].$$

From standard tables, it follows that the definite integral $\int_{1/2}^{1} \Phi^{-1}(s)ds = \frac{1}{\sqrt{2\pi}}$, so $\int_{1-\epsilon}^{1} \Phi^{-1}(s)ds = \frac{1}{\sqrt{2\pi}} - \int_{1/2}^{1-\epsilon} \Phi^{-1}(s)ds$ is continuous in ϵ and tends to 0 as ϵ tends to 0. Moreover, Φ^{-1} is strictly positive so $R(\epsilon)$ is increasing in ϵ. From standard tables it follows that

$$R(\epsilon) = \frac{1}{2\pi} e^{-\text{erfc}^{-1}(2-2\epsilon)^2},$$

where erfc is the complementary error function. Taking the inverse yields

$$R^{-1}(q) = 1 - \frac{1}{2}\sqrt{\text{erfc}(-\ln(\sqrt{2\pi}q))},$$

and a Taylor expansion of $R^{-1}(q)$ for positive q, around $q = 0$, yields

$$
\begin{aligned}
R^{-1}(q) &= -\sqrt{2}q\ln(\sqrt{2\pi}q)\left(1 + O\left(\frac{1}{-\ln(q)}\right)\right) \\
&\geq -q\sqrt{2}\ln(q\sqrt{2\pi})\left(1 - C_2\left(\frac{1}{-\ln(q)}\right)\right).
\end{aligned}
$$

Now, we have
$$\mathbb{P}\left(\|\hat{\lambda}^a - \hat{\lambda}^b\|_1 \geq 2\bar{\sigma}R(\epsilon) + C\frac{1}{N}\right) \leq 2e^{-2N\epsilon^2}.$$

29

Defining

$$q = 2\bar{\sigma} R(\epsilon) + C\frac{1}{N},$$

so that

$$\epsilon = R^{-1}\left(\frac{q - C\frac{1}{N}}{2\bar{\sigma}}\right),$$

we then get

$$\mathbb{P}\left(\|\hat{\lambda}^a - \hat{\lambda}^b\|_1 \geq q\right) \leq 2e^{-2NR^{-1}\left(\frac{q-C\frac{1}{N}}{2\bar{\sigma}}\right)^2}$$

$$\leq 2e^{-2N\left(\frac{q-C\frac{1}{N}}{2\bar{\sigma}}\right)^2 2\left(\left(-\ln\left(\sqrt{2\pi}\left(\frac{q-C\frac{1}{N}}{2\bar{\sigma}}\right)\right)\right)\left(1-C_2\frac{1}{-\ln\left(\frac{q-C\frac{1}{N}}{2\bar{\sigma}}\right)}\right)\right)^2}$$

$$= 2e^{-\frac{N}{\bar{\sigma}^2}(q-C/N)\left(\left(-\ln\left(\sqrt{2\pi}\left(\frac{q-C\frac{1}{N}}{2\bar{\sigma}}\right)\right)\right)\left(1-C_2\frac{1}{-\ln\left(\frac{q-C\frac{1}{N}}{2\bar{\sigma}}\right)^2}\right)\right)^2}$$

Note that for small positive q, for large enough N,

$$\left(-\ln\left(\sqrt{2\pi}\left(\frac{q-C\frac{1}{N}}{2\bar{\sigma}}\right)\right)\right)\left(1 - C_2\frac{1}{-\ln\left(\frac{q-C\frac{1}{N}}{2\bar{\sigma}}\right)}\right) \geq -\frac{1}{\sqrt{2}}\ln(q\sqrt{2\pi}).$$

It then follows that for such N:

$$\mathbb{P}\left(\|\hat{\lambda}^a - \hat{\lambda}^b\|_1 \geq q\right) \leq 2e^{-\frac{N}{2\bar{\sigma}^2}(q-C/N)^2\ln(q\sqrt{2\pi})^2}.$$

Now, a standard geometric series argument yields

$$2\sum_{N=1}^{\infty} e^{-\frac{N}{2\bar{\sigma}^2}(q-C/N)^2\ln(q\sqrt{2\pi})^2} < \infty,$$

and therefore, by Boole's inequality almost sure convergence follows,

$$\|\hat{\lambda}^a - \hat{\lambda}^b\|_1 \rightarrow_{a.s.} 0.$$

An identical argument for y implies that

$$\|\hat{y}^a - \hat{y}^b\|_1 \rightarrow_{a.s.} 0.$$

We then have

$$\lim_{N\to\infty}\left(\alpha\|\hat{\lambda}^a\|_1 + (1-\alpha)\|\hat{y}^a\|_1\right) - \left(\alpha\|\hat{\lambda}^b\|_1 + (1-\alpha)\|\hat{y}^b\|_1\right) = 0 \qquad a.s.,$$

and since the solution to the a-problem never has an error larger than the candidate solution with $\{\hat{\lambda}_n^a\}_n$ and $\{\hat{y}_n^a\}_n$ defined by (35,36)), it follows that

$$\limsup_{N\to\infty} E^a(N) - E^b(N) \le 0 \qquad a.s.$$

An identical argument as the one above, but instead using the permutation operator Π_a that solves the a-problem for the b-problem, with the implied $\{\hat{\lambda}_n^b\}_n$ and $\{\hat{y}_n^b\}_n$ sequences that generate a candidate solution, yields

$$\limsup_{N\to\infty} E^b(N) - E^a(N) \le 0 \qquad a.s.,$$

and therefore

$$\lim_{N\to\infty} E^b(N) - E^a(N) = 0 \qquad a.s.$$

This completes the proof of the lemma. ∎

The first part of the proposition, Equation 15, now follows directly from the fact that the actual $\{\lambda_n\}_n$ and $\{y_n\}_n$ provide a feasible solution to the b-problem. The minimal solution can, of course, never have a higher realization, so

$$E^a(N) \le \alpha\|\bar{\lambda}_{N\Delta t}\|_1 + (1-\alpha)\|\bar{y}_{N\Delta t}\|_1 + o_p(1),$$

so (15) follows.

For the second part of the proposition, Equation 16, we rewrite the b-formulation of the problem as

$$\min_{\Pi_b} \sum_n \left| \lambda_n - y_n + \sigma_n \xi_n - \sigma_n \xi_{\Pi_b(n)} \right|,$$

The estimated $\hat{\lambda}^b$ and $\hat{y}^b$ functions are then

$$\begin{aligned}
\hat{\lambda}_n^b &= \max(\lambda_n - y_n + \sigma_n(\xi_n - \xi_{\Pi_b(n)}), 0), \\
\hat{y}_n^b &= -\min(\lambda_n - y_n + \sigma_n(\xi_n - \xi_{\Pi_b(n)}), 0),
\end{aligned}$$

and the correct solutions $\hat{\lambda}^b = \lambda$ and $\hat{y}^b = y$ correspond to $\Pi_b = I$, the identity permutation operator.

Recall the condition:

Condition 1.

$$\lambda_n y_n = 0, \qquad n = 0, \ldots, N-1.$$

Consider first the case when $\sigma_n = \bar{\sigma}$, i.e., volatility is constant, so that the problem can be written

$$\min_{\Pi} \sum_n \left| \lambda_n - y_n + \bar{\sigma}(\xi_n - \xi_{\Pi(n)}) \right|. \tag{38}$$

When $\|\lambda\|_1 \leq \|y\|_1$, the bound is trivial (since then $\bar{y} \geq \|y\|_1 \geq \bar{\lambda}_{N\Delta t}$), so we focus on the interesting case when $\|\lambda\|_1 > \|y\|_1$. Note that regardless of permutation operator, if we define $r_n = \bar{\sigma}(\xi_n - \xi_{\Pi^a(n)})$, it follows that $\sum_n r_n = 0$, and the problem can be written

$$\min_{\Pi} \sum_n \left| \lambda_n - y_n + r_{\Pi(n)} \right|.$$

We have

Lemma 2. *If $\|\lambda\|_1 > \|y\|_1$ and Condition 1 is satisfied, then, define*

$$\begin{aligned}
\hat{\lambda}_n &= \max(\lambda_n + r_{\Pi(n)}, 0)1_\Lambda + \max(r_{\Pi(n)} - y_n, 0)1_Y \\
\hat{y}_n &= \max(y_n - r_{\Pi(n)}, 0)1_Y + \max(-\lambda_n - r_{\Pi(n)}, 0)1_\Lambda
\end{aligned}$$

where 1_Λ and 1_Y are the indicator functions on the sets $\Lambda = \{n : \lambda > 0\}$ and $Y = \{n : \lambda \leq 0\}$, respectively. Under these conditions,

$$\begin{aligned}
\|\hat{\lambda}\|_1 &= \|\lambda\|_1 - Z, \\
\|\hat{y}\|_1 &= \|y\|_1 - Z,
\end{aligned}$$

where $Z \leq \|y\|_1$, regardless of the permutation operator Π.

Proof of Lemma 2:
We have

$$\begin{aligned}
\|\hat{\lambda}\|_1 - \|\hat{y}\|_1 &= \sum_n \Big((\max(\lambda_n + r_{\Pi(n)}, 0) - \max(-\lambda_n - r_{\Pi(n)}, 0))1_\Lambda \\
&\quad - (\max(y_n - r_{\Pi(n)}, 0) - \max(r_{\Pi(n)} - y_n, 0))1_Y \Big) \\
&= \sum_n \Big((\max(\lambda_n + r_{\Pi(n)}, 0) + \min(\lambda_n + r_{\Pi(n)}, 0))1_\Lambda \\
&\quad - (\max(y_n - r_{\Pi(n)}, 0) + \min(y_n - r_{\Pi(n)}, 0))1_Y \Big) \\
&= \sum_n \Big((\lambda_n + r_{\Pi(n)})1_\Lambda - (y_n - r_{\Pi(n)})1_Y \Big) \\
&= \sum_n \Big(\lambda_n 1_\Lambda - y_n 1_Y - r_{\Pi(n)} \Big) \\
&= \sum_n (\lambda_n - y_n) \\
&= \|\lambda\|_1 - \|y\|_1.
\end{aligned}$$

The result then follows by defining $Z = \|\lambda\|_1 - \|\hat{\lambda}\|_1$. ∎

When applied to (38), Lemma 2 immediately implies that the solution satisfies:

$$
\begin{aligned}
\|\hat{\lambda}^b\|_1 &= \|\lambda\|_1 - Z, \\
\|\hat{y}^b\|_1 &= \|y\|_1 - Z,
\end{aligned}
$$

where $0 \leq Z \leq \|y\|_1$. We take the associated permutation operator Π as a starting point for analyzing the time-varying volatility problem, which we rewrite as

$$
\min_{\Pi_b} \sum_n \left| \lambda_n - y_n + \bar{\sigma}(\xi_n - \xi_{\Pi_b(n)}) + \Delta\sigma_n(\xi_n - \xi_{\Pi_b(n)}) \right|, \tag{39}
$$

where $\bar{\sigma}$ denotes the time series mean of $\{\sigma_n\}_n$, and $\{\Delta\sigma_n\}_n$ denotes the sequence of deviations from that mean. Of course, Π is a candidate solution permutation operator to the problem. If a better permuation operator Π^b exists, the improvement of using Π_b over Π then must come from the terms

$$
X_n^{\Pi_b} \overset{\text{def}}{=} \Delta\sigma_n(\xi_n - \xi_{\Pi_b(n)}).
$$

Define the sample mean of this variable:

$$
\bar{X}^{\Pi_b} = \frac{1}{N} \sum_n X_n^{\Pi_b}.
$$

Now, since ξ_n is independent of σ_n, and σ_n is bounded above, the weak law of large numbers implies that

$$
\frac{1}{N} \sum_n \Delta\sigma_n \xi_n = o_p(1),
$$

and thus

$$
\bar{X}^{\Pi_b} = -Q + o_p(1),
$$

where

$$
Q = \frac{1}{N} \sum_n \Delta\sigma_n \xi_{\Pi_b(n)}.
$$

The trade-off of moving from the permutation operator Π which is optimal under constant volatility, to Π_b which is globally optimal, is now between the increasing effect from the middle part of (39) — the part multiplied by $\bar{\sigma}$) — and the decreasing effect from the rightmost part — which depends on $\{X_n^{\Pi_b}\}_n$.

Now, consider the solution to (39), with permutation operator Π_b, and define the estimates $\{\check{\lambda}_n^b\}_n$, and $\{\check{y}_n^b\}_n$ as those in the average volatility formulation (38) under the Π_b permutation operator. Obviously,

$$
\|\check{\lambda}^b\|_1 + \|\check{y}^b\|_1 > \|\hat{\lambda}^b\|_1 + \|\hat{y}^b\|_1,
$$

since the Π_b permutation operator is not designed to minimize the error under constant volatility,

whereas Π is. It also follows that

$$\frac{1}{N}\sum_n \left| \check{\lambda}_n - \check{y}_n^b + \bar{\sigma}(\xi_n - \xi_{\Pi_b(n)}) + \Delta\sigma_n(\xi_n - \xi_{\Pi_b(n)}) \right| = \frac{1}{N}\sum_n \left| \lambda_n^b - y_n^b + X_n^{\Pi_b} \right|$$

$$\geq \|\check{\lambda}^b\|_1 + \|\check{y}^b\|_1 + X^{\Pi_b},$$

since by decomposing $\{0,\ldots,N-1\} = \Lambda \cup Y$, where $\Lambda = \{n : \check{\lambda}^b > 0\}$, $Y = \{n : \check{\lambda}^b \leq 0\}$, it follows that

$$\begin{aligned}
\|\lambda^b\|_1 + \|y^b\|_1 &= \frac{1}{N}\sum_n \left| \check{\lambda}_n^b - \check{y}_n^b + X_n^{\Pi_b} \right| \\
&= \frac{1}{N}\sum_{n\in\Lambda} \left| \check{\lambda}_n^b + X_n^{\Pi_b} \right| + \frac{1}{N}\sum_{n\in Y} \left| -\check{y}_n^b + X_n^{\Pi} \right| \\
&\geq \frac{1}{N}\sum_{n\in Y} (\check{\lambda}_n^b + X_n^{\Pi}) + \frac{1}{N}\sum_{n\in Y} (-\check{y}_n^b + X_n^{\Pi}) \\
&= \|\check{\lambda}^b\|_1 + \|\check{y}^b\|_1 + X^{\Pi_b} \\
&\geq \|\hat{\lambda}^b\|_1 + \|\hat{y}^b\|_1 + X^{\Pi_b} \\
&\geq \|\lambda\|_1 + \|y\|_1 - 2Z + X^{\Pi_b} \\
&= \|\lambda\|_1 + \|y\|_1 - 2Z - Q + o_p(1).
\end{aligned}$$

It follows that

$$\|\lambda\|_1 \leq \|\lambda^b\|_1 + \|y^b\|_1 - \|y\|_1 + 2Z + Q + o_p(1).$$

Now, since $Z \leq \|y\|_1$, and $\|y\|_1 \leq \bar{y}$, we have $-\|y\|_1 + 2Z \leq \bar{y}$. Moreover, $\|\lambda^a\|_1 + \|y^a\|_1 = \|\lambda^b\|_1 + \|y^b\|_1 + o_p(1)$ by Lemma 1, and by the law of large numbers

$$\begin{aligned}
Q^N \stackrel{\text{def}}{=} \frac{1}{N}\sum_n \sigma_n \hat{\xi}_{\Pi_b(n)} &= \frac{1}{N}\sum_n \Delta\sigma_n \hat{\xi}_{\Pi_b(n)} \\
&= \frac{1}{N}\sum_n \Delta\sigma_n \xi_{\Pi_b(n)} + o_p(1) \\
&= Q + o_p(1)
\end{aligned}$$

where the first equality follows from the fact that $\sum_n \hat{\xi}_{\Pi_b(n)} = 0$ (because of the symmetric choice of the G function). This takes us to:

$$\begin{aligned}
\|\lambda\|_1 &\leq \|\lambda^b\|_1 + \|y^b\|_1 - \|y\|_1 + 2Z + Q + o_p(1) \\
&\leq \|\lambda^a\|_1 + \|y^a\|_1 + \bar{y} + Q^N + o_p(1),
\end{aligned}$$

i.e., we have shown (16).

When the condition $\lambda_n y_n = 0$ for all n is not satisfied, we can repeat the whole argument above, with the adjusted coefficients $\tilde{\lambda}_n = \max(\lambda_n - y_n, 0)$ and $\tilde{y}_n = \max(y_n - \lambda_n, 0)$, which do satisfy the

condition $\tilde{\lambda}_n \tilde{y}_n = 0$, and also $\|\tilde{\lambda}\| \leq \|\lambda\|$ and $\|\tilde{y}\| \leq \|y\| \leq \bar{y}$. This then implies:

$$\|\tilde{\lambda}\|_1 \quad \leq \quad \|\lambda^a\|_1 + \|y^a\|_1 + \bar{y} + Q^N + o_p(1).$$

We also have $\|\tilde{\lambda}\|_1 + \|\tilde{y}\|_1 \geq \|\lambda\|_1 - \|y\|_1 \geq \|\lambda\|_1 - \bar{y}$, so $\|\tilde{\lambda}\|_1 \geq \|\lambda\|_1 - 2\bar{y}$. Using this inequality, we get

$$\|\lambda\|_1 - 2\bar{y} \leq \|\tilde{\lambda}\|_1 \leq \|\lambda^a\|_1 + \|y^a\|_1 + \bar{y} + Q^N + o_p(1),$$

which takes us to (17). We are done.

$\blacksquare$

B Matlab code for CVP

```
%% CVP Matlab code, JW, March 2, 2022
%% Input:
%% - r:  Per period discount rate
%% - rt:  Per period returns
%% - sigT: Per period volatility
%% - ybar:  Maximum average yield
%% - alpha:  Weight in optimization
%% Output:
%% -Lhat:  Upper survival probability
%% -Lcheck:  Lower survival probability
%% -lambdaMean:  Mean of lambda
%% -yMean:  Mean y
function [Lhat,Lcheck,lambdaMean,yMean] = CVP(r,rt,sigT,ybar,alpha)
if size(rt,1)>1 %Want row vector
rt=rt';
end
if size(sigT,1)>1 %Want row vector
sigT=sigT';
end
T = length(rt);
ER=rt-r; %Excess return
XI=ER./sigT; %Normalized excess returns
G=norminv(1/(T+1)*(1:T)); % Inverse normal vector
%Cost function
C=zeros(T,T);
p=1; %Which norm (1 in paper)
for k=1:T
for j =1:T
  z0=alpha*(ER(k)-sigT(k)*G(j)>0)+(1-alpha)*((ER(k)-sigT(k)*G(j)<0));
  C(k,j)=z0*abs(ER(k)-sigT(k)*G(j))^p;
end;
end;
a=matchpairs(C,100);a=a(:,1); %First column is permutation map
b=zeros(T,1);for nn=1:T b(a(nn))=nn;end %Inverse permutation
DLOpt=(XI-G(b)).*sigT; %Minimized realizations
Lambda=DLOpt.*(DLOpt>0);
lambdaMean = sum(Lambda)/T;
Y=-DLOpt.*(DLOpt<0);
yMean = sum(Y)/T;
Lhat = exp(-lambdaMean*T);
QN=sum(sigT.*G(b))/T;
Lcheck = exp(-(lambdaMean+yMean+ybar+QN)*T);
```

References

Allen, F., S. Morris, and A. Postlewaite. 1993. Finite bubbles with short sale constraints and asymmetric information. *Journal of Economic Theory* 61:206–229.

Astill, S., D. I. Harvey, S. J. Leybourne, A. Taylor, and Y. Zu. 2021. CUSUM-based monitoring for explosive episodes in financial data in the presence of time-varying volatility. *Journal of Financial Econometrics* .

Athey, S., I. Parashkevov, V. Sarukkai, and J. Xia. 2016. Bitcoin pricing, adoption, and usage: Theory and evidence. *Stanford GSB Working paper 3469* URL https://ssrn.com/abstract=2826674.

Biais, B., C. Bisiére, M. Bouvard, C. Casamatta, and A. J. Menkveld. 2020. Equilibrium Bitcoin pricing. *Journal of Finance, forthcoming* .

Bjork, T. 2011. An Introduction to Point Processes from a Martingale Point of View. Royal Institute of Technology, Stockholm, Sweden.

Blanchard, O. J. 1979. Speculative bubbles, crashes and rational expectations. *Economics Letters* 3:387–389.

Cheah, E.-T., and J. Fry. 2015. Speculative bubbles in Bitcoin markets? An empirical investigation into the fundamental value of Bitcoin. *Economics Letters* 130:32–36.

Choi, K. J., A. Lehar, and R. Stauffer. 2018. Bitcoin microstructure and the Kimchi premium. *SSRN Working paper* URL https://ssrn.com/abstract=3189051.

Cong, L. W., Y. Li, and N. Wang. 2021. Tokenomics: Dynamic adoption and valuation. *Review of Financial Studies* 34:1105–1155.

Foley, S., J. Karlsen, and T. J. Putniņš. 2019. Sex, drugs, and bitcoin: How much illegal activity is financed through cryptocurrencies? *Review of Financial Studies* 32:1798–1853.

Froot, K. A., and M. Obstfeld. 1991. Intrinsic Bubbles: the case of stock prices. *American Economic Review* 81:1189–1214.

Gandal, N., J. Hamrick, T. Moore, and T. Oberman. 2018. Price manipulation in the Bitcoin ecosystem. *Journal of Monetary Economics* 95:86–96.

Griffin, J. M., and A. Shams. 2018. Is Bitcoin really untethered? *Journal of Finance* 75:1913–1964.

Harvey, D., S. Leybourne, and Y. Zu. 2020. Sign-based unit root tests for explosive financial bubbles in the presence of deterministically time-varying volatility. *Econometric Theory* 36:122–169.

Harvey, D. I., S. J. Leybourne, R. Sollis, and A. M. R. Taylor. 2016. Tests for explosive financial bubbles in the presence of non-stationary volatility. *Journal of Empirical Finance* 38:548–574.

Harvey, D. I., S. J. Leybourne, and Y. Zu. 2018. Testing explosive bubbles with time-varying volatility. *Econometric Reviews* 38:1131–1151.

Kaminsky, G. 1993. Is there a Peso problem? Evidence from the dollar/pound exchange rate 1976-1987. *American Economic Reveiew* 83:450–472.

Krasker, W. S. 1980. The 'peso problem' in testing the efficiency of forward exchange markets. *Journal of Monetary Economics* 6:269–276.

Liu, Y., and A. Tsyvinsky. 2021. Risks and returns of cryptocurrency. *Review of Financial Studies* 34:2689–2727.

Lizondo, J. S. 1983. Foreign exchange futures prices under fixed exchange rates. *Journal of International Economics* 14:69–84.

Makarov, I., and A. Schoar. 2020. Trading and arbitrage in cryptocurrency markets. *Journal of Financial Economics* 135:293–319.

Massart, P. 1990. The tight constant in the Dvoretzky-Kiefer-Wolfowitz inequality. *Annals of Probability* 18:1269–1283.

Merton, R. C. 1976. Option Pricing When Underlying Stock Returns are Discontinuous. *Journal of Financial Economics* 3:125–144.

Pagnotta, E. S. 2022. Decentralizing money: Bitcoin prices and blockchain security. *The Review of Financial Studies* 35:866–907.

Pagnotta, E. S., and A. Buraschi. 2018. An equilibrium valuation of Bitcoinand decentralized network assets. Working paper, Imperial College Business School.

Pastor, L., and P. Veronesi. 2006. Was there a Nasdaq bubble in the late 1990s? *Journal of Financial Economics* 81:61–100.

Phillips, P. C. B., S. Shi, and J. Yu. 2014. Specification sensitivity in right-tailed unit root testing for explosive behavior. *Oxford Bulletin of Economics and Statistics* 76:315–333.

Phillips, P. C. B., S. Shi, and J. Yu. 2015a. Testing for multiple bubbles: Limit theory of real-time detectors. *International Economic Review* 56:1079–1134.

Phillips, P. C. B., S. P. Shi, and J. Yu. 2015b. Testing for multiple bubbles: Historical episodes of exuberance and collapse in the S&P 500. *International Economic Review* 56:1043–1078.

Phillips, P. C. B., Y. Wu, and J. Yu. 2011. Explosive behavior in the 1990s Nasdaq: When did exuberance escalate asset value? *International Economic Review* 52:201–226.

Rogoff, K. 1977. Rational expectations in the foreign exchange market revisited. Unpublished manuscript, MIT.

Rogoff, K. 1980. Tests of the martingale model for foreign exchange markets futures markets, in Essays on expectations and exchange rate volatility. Ph.D. Thesis, MIT.

Schuh, S., and O. Shy. 2015. US consumers adoption and use of Bitcoin and other virtual currencies. Working paper, MIT Sloan School of Management.

Shi, S., and P. C. B. Phillips. 2021. Econometric analysis of asset price bubbles. URL `https://drive.google.com/open?id=13WZenaHho63enhm0eYX145v-uGX6s87a`. Working paper, Yale University.

Shiller, R. J. 1981. Do stock prices move too much to be justified by subsequent changes in dividends. *American Economic Review* 71:421–436.

Shiller, R. J. 2000. *Irrational Exuberance.* Princeton University Press.

Shiller, R. J. 2014. Speculative Asset Prices. *American Economic Review* 104:1486–1517.

Skrobotov, A. 2021. Testing for Explosive Bubbles: A Review. URL `https://ssrn.com/abstract=3779111`. SSRN Working paper.

Sockin, M., and W. Xiong. 2018. A Model of Cryptocurrencies. URL `https://ssrn.com/abstract=3550965`. NBER Working Paper No. w26816.

Urquhard, A. 2016. The inefficiency of Bitcoin. *Economic Letters* 148:80–82.
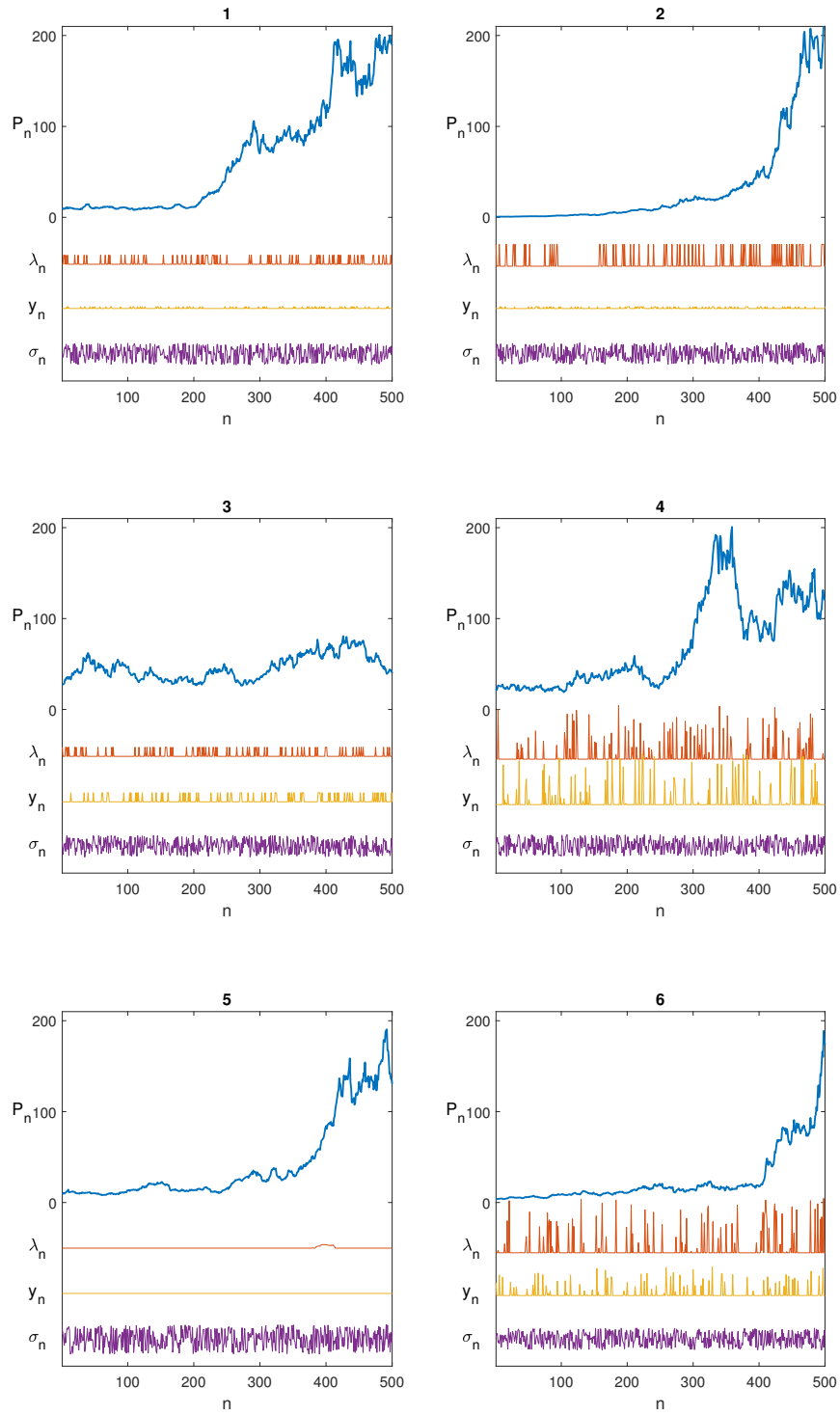
Figure 2: **Benchmark problems in panels 1,3, and 5, are consistent with fundamental prices. Benchmark problems in panels 2, 4 and 6 not consistent.**
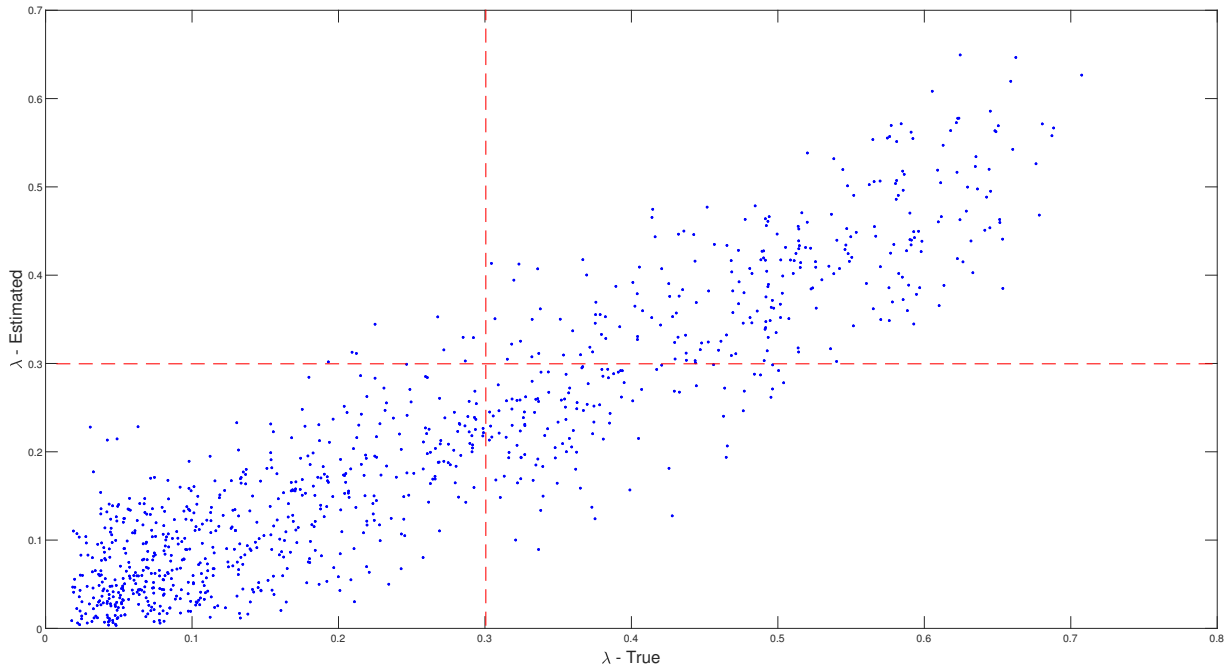
Figure 3: **Actual and estimated λ in simulations, on x-axis and y-axis, respectively. Of 1000 simulations, 613 correctly classified as consistent with fundamental value pricing ($\lambda < 0.30$), 258 correctly classified as inconsistent ($\lambda \geq 0.30$), 120 are incorrectly classified as consistent, and 9 are incorrectly classified as inconsistent. Parameters: $r = 0.1$, average volatility 0.28.**
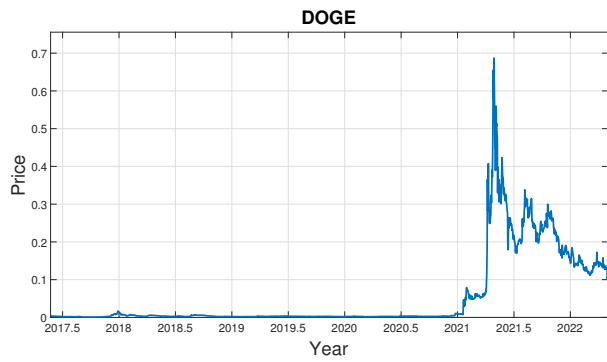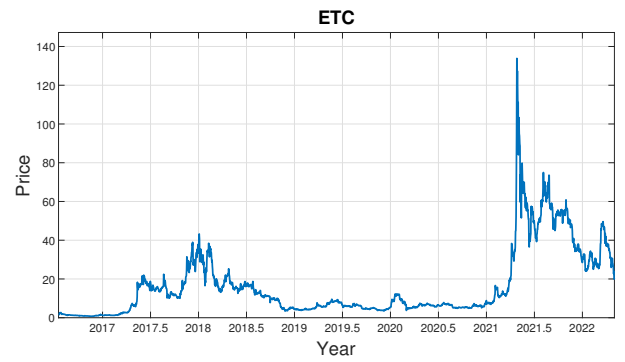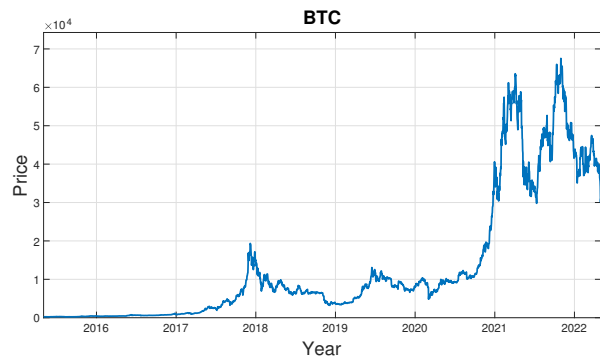
Figure 4: **Price dynamics and volatility of Bitcoin (BTC), Ethereum Classic (ETC), Dogecoin (DOGE), and Stellar (XLM).**
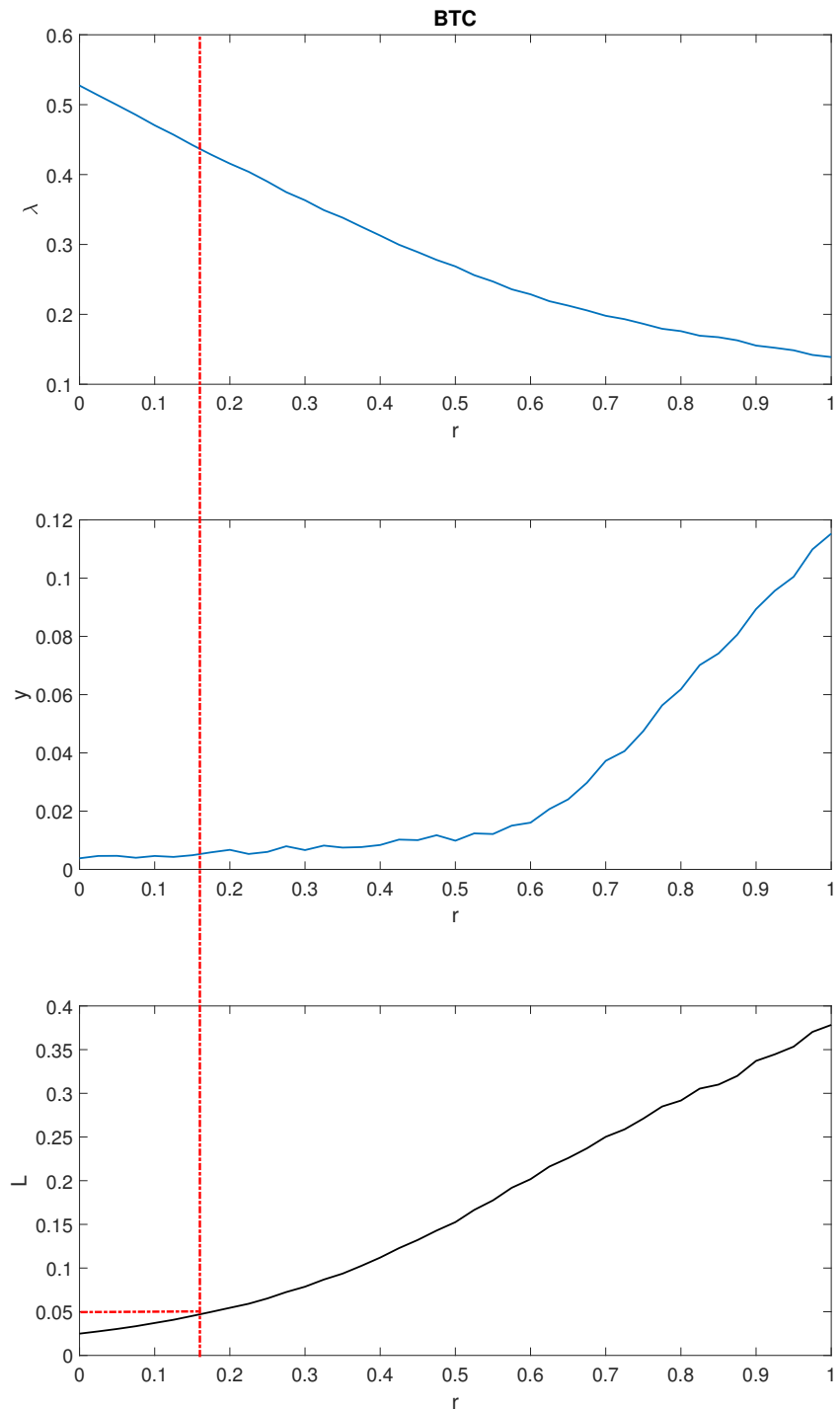
Figure 5: **Bitcoin (BTC) estimation: Fundamental value pricing consistent at survival probability** $L = 5\%$, **with** $r \geq 0.18$ **and yield** $y \geq 0.005$ **per year.**
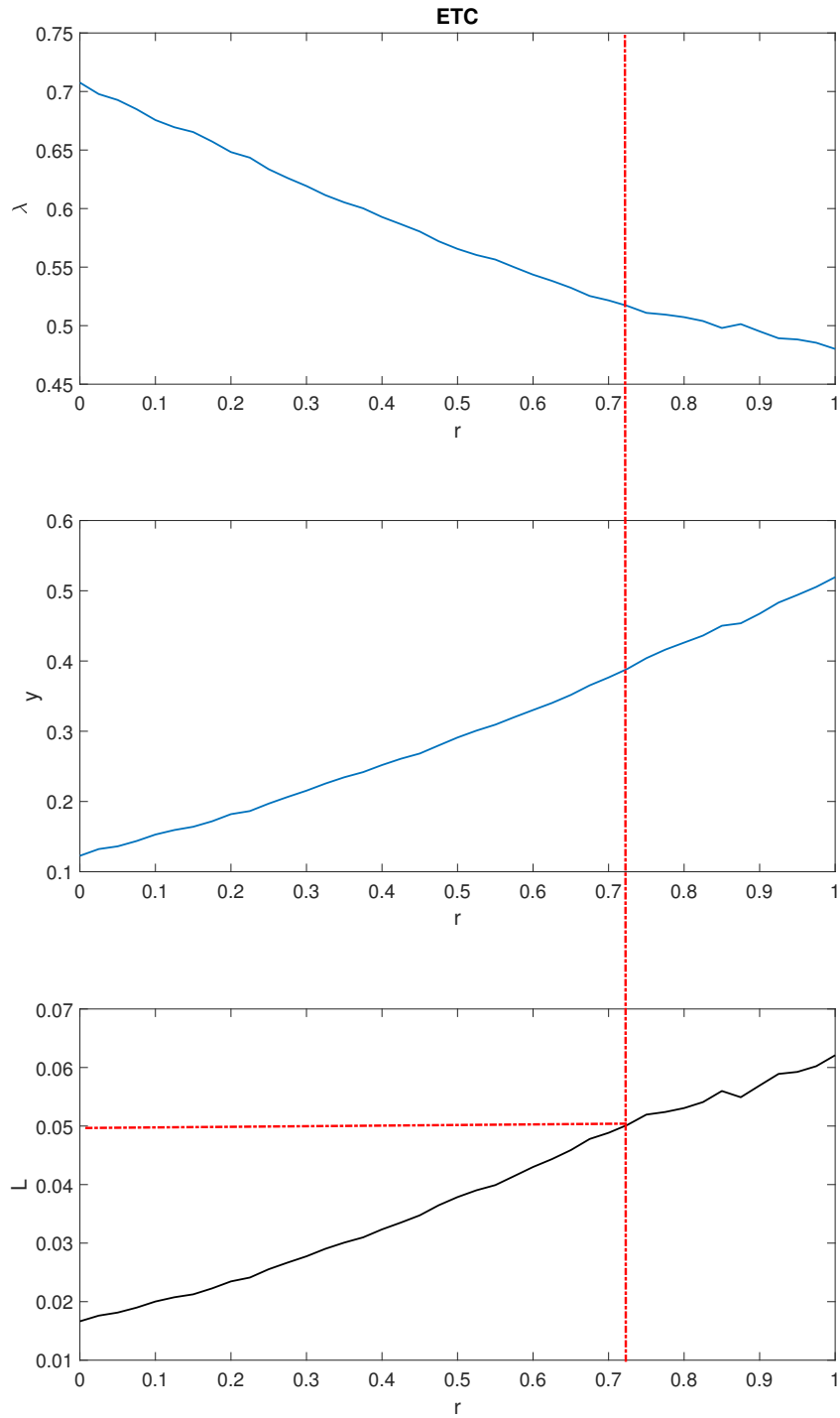
Figure 6: **Ethereum Classic (ETC) estimation: Dynamics consistent with fundamental value pricing at survival probability $L = 5\%$, with $r \geq 0.0.72$, and yield $y \geq 0.35$ per year.**
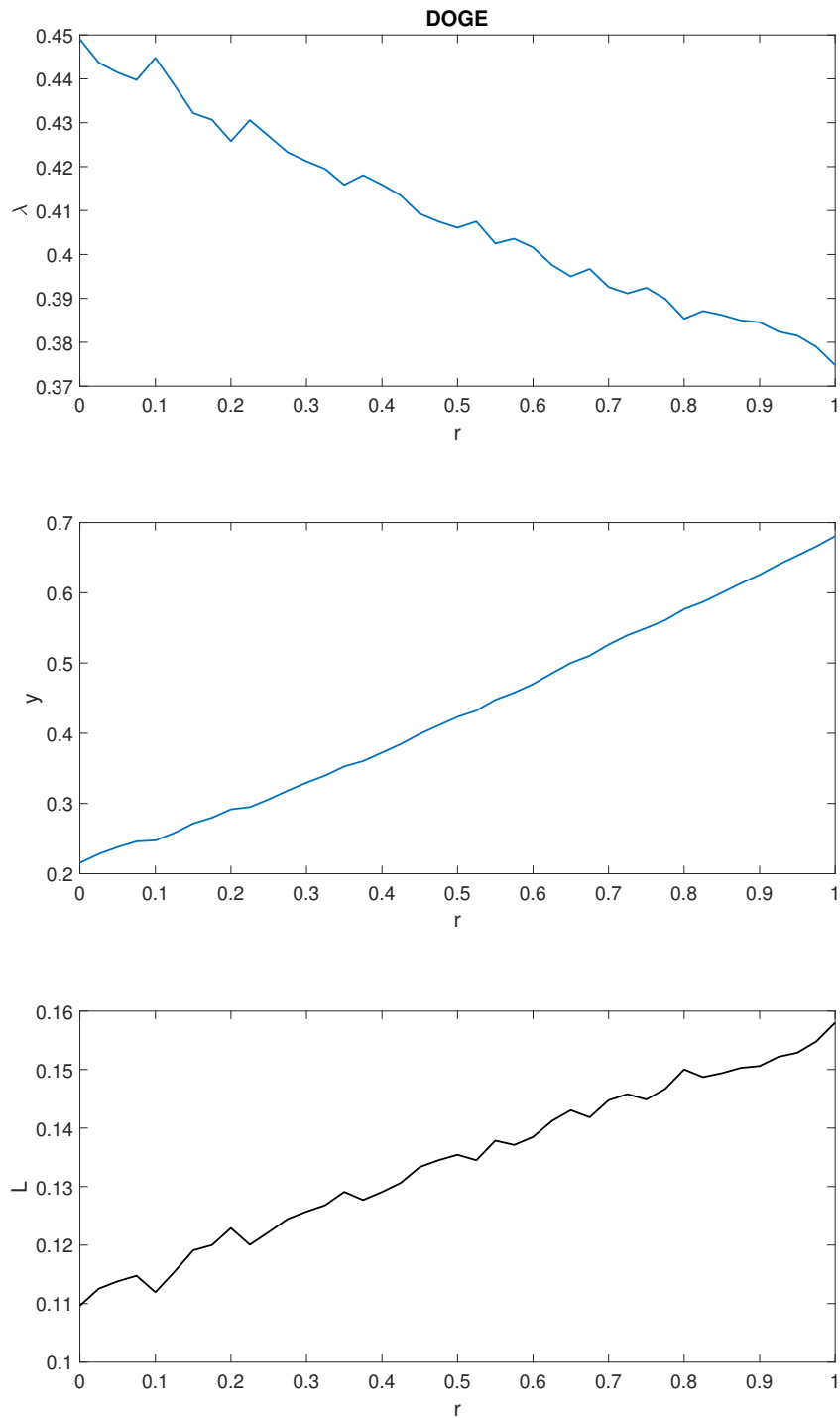
Figure 7: **Dogecoin (DOGE) estimation: Fundamental value pricing consistent at survival probability $L = 5\%$, with $r \geq 0$ and yield $y \geq 0.21$ per year.**
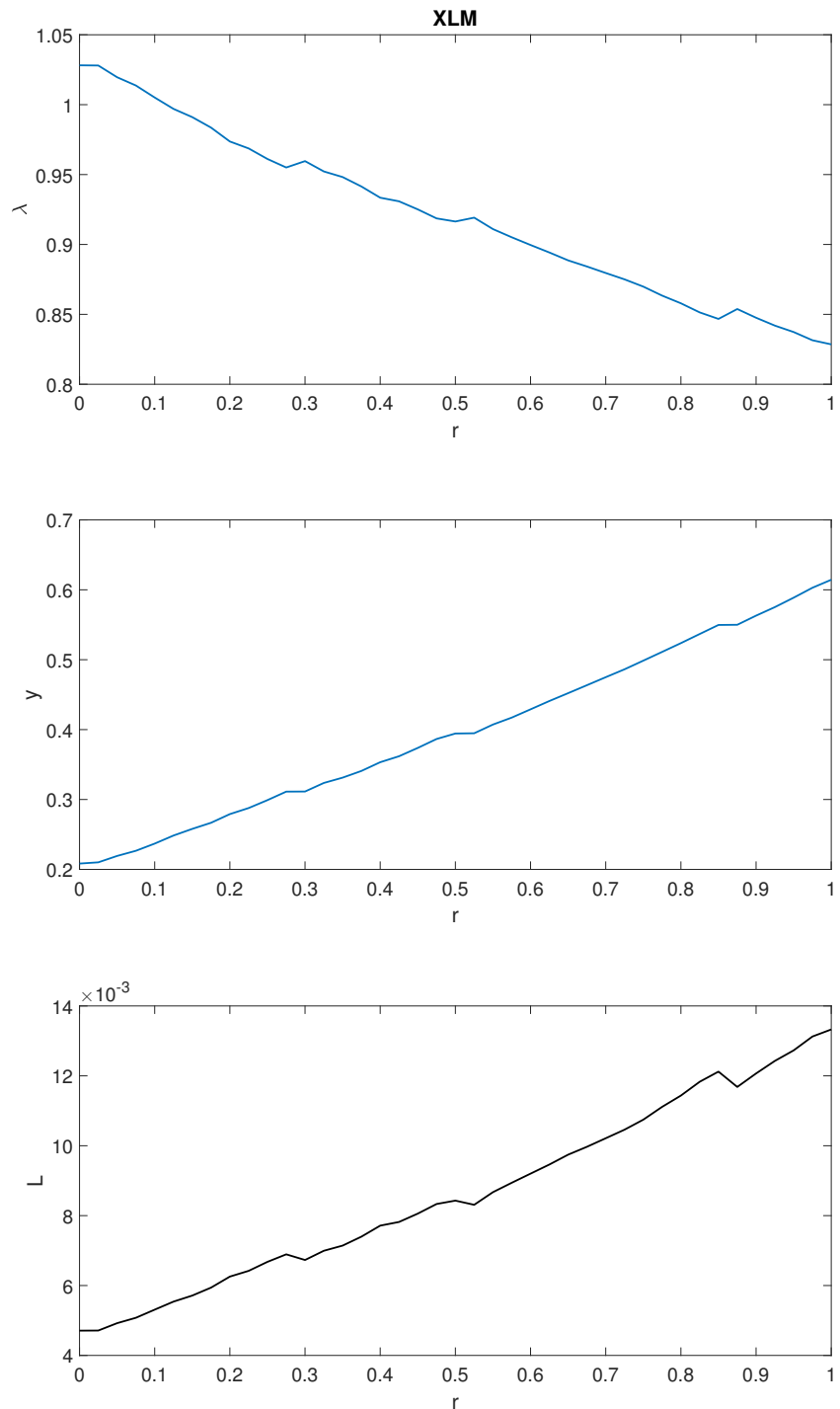
Figure 8: **Stellar (XLM) estimation: Fundamental value pricing not consistent at survival probability** $L = 5\%$, **for any** $r \leq 1$.